

1 **Pulses of enhanced continental weathering associated with multiple Late**
2 **Devonian climate perturbations: Evidence from osmium-isotope**
3 **compositions**

4
5 L.M.E. Percival^{1±*}, D. Selby^{2,3}, D.P.G. Bond⁴, M. Rakociński⁵, G. Racki⁵, L. Marynowski⁵, T. Adatte¹, J.E.
6 Spangenberg⁶, K.B. Föllmi¹

7
8 *1: Institute of Earth Sciences, University of Lausanne, Géopolis, 1015 Lausanne, Switzerland*

9 *2: Department of Earth Sciences, Durham University, Durham, DH1 3LE, UK*

10 *3: State Key Laboratory of Geological Processes and Mineral Resources, School of Earth Resources, China*
11 *University of Geosciences, Wuhan, 430074 Hubei, China*

12 *4: Department of Geography, Geology and Environment, University of Hull, Cottingham Road, Hull, HU6 7RX,*
13 *UK*

14 *5: Faculty of Earth Sciences, University of Silesia, Będzińska 60, 41-200 Sosnowiec, Poland*

15 *6: Institute of Earth Surface Dynamics, University of Lausanne, Géopolis, 1015 Lausanne, Switzerland*

16 *±: Current address – Analytical, Environmental and Geochemistry Group, Vrije Universiteit Brussel, 1050*
17 *Brussels, Belgium*

18 **Corresponding author e-mail – lawrence.percival11@gmail.com*

19
20 **KEYWORDS:**

21 **Frasnian–Famennian extinction; Kellwasser horizons; Annulata event; nutrient runoff;**
22 **marine anoxia; Kowala quarry**

23
24 **ABSTRACT**

25 **Anomalously high rates of continental weathering have frequently been proposed**
26 **as a key stimulus for the development of widespread marine anoxia during a number of**
27 **Late Devonian environmental and biospheric crises, which included a major mass**

28 extinction during the Frasnian–Famennian transition (marked by the Upper and Lower
29 Kellwasser horizons). Here, this model is investigated by presenting the first stratigraphic
30 record of osmium-isotope trends ($^{187}\text{Os}/^{188}\text{Os}$) in upper Devonian strata from the Kowala
31 Quarry (Holy Cross Mountains, Poland). Changes in reconstructed $^{187}\text{Os}/^{188}\text{Os}$ seawater
32 values to more radiogenic compositions are documented at the base of both the Lower
33 (~0.42 to ~0.83) and Upper (~0.31 to ~0.81) Kellwasser horizons characteristic of the
34 Frasnian–Famennian transition, and additionally within upper Famennian shales that
35 record a more minor environmental perturbation known as the Annulata Event (~0.20 to
36 ~0.53). These shifts indicate the occurrence of extremely enhanced continental
37 weathering rates at the onsets of the Kellwasser crises and during the later Annulata
38 Event. The similarity of $^{187}\text{Os}/^{188}\text{Os}$ values in this study from Frasnian–Famennian
39 boundary and lower Famennian strata (between 0.4–0.5) to those from North American
40 stratigraphic equivalents suggests that the $^{187}\text{Os}/^{188}\text{Os}$ values record global trends. These
41 findings support a causal relationship between increased continental weathering (and
42 thus, nutrient supply to the marine shelf) and the environmental perturbations that
43 occurred during numerous Late Devonian events, including both of the biospherically
44 catastrophic Kellwasser crises as well as other, less severe, oceanic anoxic events.

45

46

47 1. Introduction

48

49 The Late Devonian (~383–359 Ma) marked a time of numerous environmental and biotic
50 crises, including one of the ‘Big Five’ mass extinctions of the Phanerozoic Aeon during the Frasnian–
51 Famennian (F–F) transition (see reviews in Racki, 2005; Bond and Grasby, 2017). Although the
52 magnitude of extinction and/or environmental perturbation appears to have greatly varied between the
53 Late Devonian crises, a common feature of these events was the development of widespread marine

54 anoxia, typically recorded by the appearance of organic-rich laminated shales in the stratigraphic record
55 (e.g., Joachimski and Buggisch, 1993; Walliser, 1996; Bond *et al.*, 2004; Racka *et al.*, 2010; Becker *et*
56 *al.*, 2016; Bond and Grasby, 2017). Two such anoxic episodes are documented to have occurred during
57 the late Frasnian, widely known as the Lower (LKW) and Upper (UKW) Kellwasser events (~372 Ma),
58 the latter of which coincided with the F–F transition and the associated mass extinction. Subsequent
59 spells of marine anoxia during the Famennian Stage included the Annulata (~363 Ma) and Hangenberg
60 (~359 Ma) events at the end of the Devonian Period, with the Hangenberg Event characterized by
61 another major mass extinction (see reviews by Kaiser *et al.*, 2016; and Bond and Grasby, 2017). The
62 ultimate causes of the various Late Devonian environmental perturbations remain debated. Numerous
63 triggers have been postulated for the Kellwasser crises, including extra-terrestrial impacts (e.g., Wang,
64 1992; Claeys *et al.* 1996; Du *et al.*, 2008), large-scale volcanic activity potentially linked to the Viluy
65 Traps in Siberia (e.g., Courtillot *et al.*, 2010; Ricci *et al.*, 2013; Racki *et al.*, 2018), orogenic uplift and
66 erosion (Averbuch *et al.*, 2005), and the expansion of vascular-rooted terrestrial flora (Algeo *et al.*,
67 1995; Algeo and Scheckler, 1998). Many of the environmental perturbations also appear to have
68 coincided with climate cooling (e.g., StreeL *et al.*, 2000; Joachimski and Buggisch, 2002; Balter *et al.*,
69 2008). The Annulata anoxic event was coeval with a major marine transgression (Johnson *et al.*, 1985),
70 and may also have coincided with a major pulse of volcanic activity (Percival *et al.*, 2018). In contrast,
71 Southern-Hemisphere glaciation, and associated continental weathering and marine regression, has been
72 most frequently proposed as having caused the end-Famennian Hangenberg Event (e.g., StreeL *et al.*,
73 2000; Kaiser *et al.*, 2016; Lakin *et al.*, 2016). Whatever initiated the various Late Devonian crises and
74 caused any associated extinctions, in all cases the development of marine anoxia has been proposed to
75 have been driven by internal triggers. One such postulated trigger is an enhancement of global
76 weathering rates and an associated flux of nutrients to the marine realm, which stimulated increased
77 primary productivity and consumption of oxygen in the water column (e.g., Wilder, 1994; Algeo *et al.*,
78 1995; Algeo and Scheckler, 1998; Averbuch *et al.*, 2005; Chen *et al.*, 2005; Whalen *et al.*, 2015).

79
80 This study presents a new long-term stratigraphic record of sedimentary osmium (Os) isotopes
81 (specifically $^{187}\text{Os}/^{188}\text{Os}$) from rocks that span mid Frasnian up to upper Famennian strata (that

82 represent approximately 20 million years of Late Devonian time). The $^{187}\text{Os}/^{188}\text{Os}$ composition of
83 sedimentary rocks can track changes in both continental weathering rates and the influx of
84 mantle/meteorite material into the global oceans, due to proportional mixing of inputs to the oceanic
85 inventory from extra-terrestrial and mantle-derived-volcanic osmium ($^{187}\text{Os}/^{188}\text{Os}$ of 0.13: Allègre *et al.*,
86 *1999*) and the riverine supply of the element from weathering of the continental crust (average
87 $^{187}\text{Os}/^{188}\text{Os}$ of ~ 1.4 : Peucker-Ehrenbrink and Jahn, 2001). The marine residence time of Os (10–50 kyr
88 or less; Peucker-Ehrenbrink and Ravizza, 2000; Rooney *et al.*, 2016) results in a homogeneous Os-
89 isotope composition throughout the open ocean. Hydrographically restricted basins may have different
90 seawater Os-isotope values, determined by local sources of the element, if their water-mixing time with
91 the global ocean is longer than the lifetime of marine Os (Paquay and Ravizza, 2012; Du Vivier *et al.*,
92 2014; Dickson *et al.*, 2015; Percival *et al.*, 2016). Past seawater Os-isotope compositions ($\text{Os}_{(i)}$) can be
93 calculated from a sedimentary rock after accounting for radiogenic ^{187}Os produced from post-deposition
94 decay of ^{187}Re (rhenium), assuming that the sedimentary system has remained closed with respect to Re
95 and Os, and that the age of the studied sample is known (Cohen *et al.*, 1999).

96
97 Previous studies of Late Devonian sedimentary records have utilized Re–Os isochrons (based
98 on the known half-life of the decay of ^{187}Re to ^{187}Os) to date organic-rich strata from a number of North
99 American sequences (Figure 1). This technique can also determine the isotopic composition of the
100 sediment at the time of deposition ($\text{Os}_{(i)}$), and thus, for an open-marine palaeoenvironment, the Os-
101 isotope signature of the global ocean at that specific time. Following these investigations, the Late
102 Devonian (particularly Famennian) ocean is considered to have had an average $^{187}\text{Os}/^{188}\text{Os}$ composition
103 of ~ 0.46 (Figure 2), with values of ~ 0.45 and 0.42 measured at the Frasnian–Famennian and Devonian–
104 Carboniferous (D–C) boundaries, respectively (Selby and Creaser, 2005; Turgeon *et al.*, 2007; Gordon
105 *et al.* 2009; Harris *et al.*, 2013). However, trends in Os-isotope values across the stratigraphic sequences
106 of specific Late Devonian events, such as the Kellwasser crises, have not been previously documented.
107 Consequently, it is unknown how the global Os inventory responded to possible influences from any or
108 all of the postulated meteorite impacts, volcanic activity, or enhanced continental weathering rates
109 thought to have occurred during the various Late Devonian environmental perturbations (e.g., Wang,

110 1992; Claeys *et al.*, 1996; Algeo and Scheckler, 1998; Averbuch *et al.*, 2005; Chen *et al.*, 2005;
111 Courtillot *et al.*, 2010; Ricci *et al.*, 2013; Whalen *et al.*, 2015; Racki *et al.*, 2018).

112
113 The Kowala Quarry (hereafter termed Kowala), near the town of Kielce in the Holy Cross
114 Mountains, Poland, records a well-known long-term record of the Late Devonian, with strata from the
115 lower Frasnian through to basal Tournasian (Early Carboniferous) series well constrained by conodont
116 biostratigraphy (Szulczewski, 1996; see figure 1 in De Vleeschouwer *et al.*, 2013). The sediments were
117 deposited in the Chęciny–Zbrza intra-shelf basin, which was surrounded by more elevated shoal areas
118 that formed part of a very large carbonate platform on the north-eastern part of Laurentia (Figure 1, see
119 also review by Racki *et al.*, 2002). The presence of conodont fossils found across Europe, North
120 America, and South China (Szulczewski, 1971, 1996) indicates that marine organisms could certainly
121 migrate between the basin and global ocean, although the degree of connectivity between those two
122 environments in terms of water-mass mixing remains unknown. Organic-rich shales (interbedded with
123 limestones) are prevalent throughout much of the Kowala stratigraphic sequence, ideal for Re–Os
124 analysis due to the uptake of both Re and Os from seawater into organic muds during deposition
125 (Ravizza and Turekian, 1989; Cohen *et al.*, 1999). The UKW Horizon has been well documented at
126 Kowala on the basis of conodont biostratigraphy (Szulczewski, 1971, 1996), an elevated total organic
127 carbon (TOC) content, and a positive carbon-isotope ($\delta^{13}\text{C}$) excursion of up to 4 ‰ in both carbonates
128 and bulk and compound-specific organic matter (Joachimski *et al.*, 2001), which is characteristic of
129 both Kellwasser events in stratigraphic archives across the globe (e.g., Joachimski and Buggisch, 1993;
130 Chen *et al.*, 2005; De Vleeschouwer *et al.*, 2017). This stratigraphic positioning of the UKW Horizon is
131 supported by several other indications of marine anoxia such as pyrite framboid size populations and
132 trace metal contents (e.g., vanadium/chromium ratios), all of which show perturbations just below the
133 F–F boundary (Joachimski *et al.*, 2001; Racki *et al.*, 2002; Bond *et al.*, 2004). The position of the LKW
134 Horizon has been inferred previously from the appearance of organic-rich shales about 10 metres below
135 the UKW Horizon in the Late *rhenana* conodont Zone, consistent with other western European records
136 and supported by lithological evidence for marine anoxia, although the positive $\delta^{13}\text{C}$ excursion
137 characteristic of the LKW Horizon is not well defined at Kowala (Joachimski *et al.*, 2001; Bond *et al.*,

138 2004). Several Famennian episodes of marine anoxia/euxinia are also well known from the appearance
139 of black shale horizons higher in the Kowala Quarry sequence, with both the Annulata and Hangenberg
140 Events recorded (e.g., Bond and Zatoń, 2003; Racka *et al.*, 2010; Marynowski *et al.*, 2012).

141
142 For this study, sedimentary rocks from both Kellwasser horizons and the Annulata and
143 Hangenberg shales at Kowala, together with sediments from seven Frasnian and Famennian
144 stratigraphic levels that were deposited between the times of the individual Late Devonian events, were
145 analyzed to determine their Os_(i) compositions. New samples were taken from throughout the Kowala
146 stratigraphic sequence in September 2017 (including the Lower Kellwasser, Annulata, and Hangenberg
147 shales), and combined with rocks from an unpublished sample-set spanning the F–F boundary,
148 collected in 2009 by Michal Rakociński and Leszek Marynowski (part of the Global Archive of
149 Devonian System Samples at the University of Silesia, Sosnowiec, Poland). Where possible, the results
150 were compared to Os_(i) values in rocks from time-equivalent strata in North America. Because Kowala
151 is an active quarry, it is no longer possible to sample the exact section studied by Joachimski *et al.*
152 (2001); therefore, $\delta^{13}\text{C}$, TOC, and trace-metal data were also determined for uppermost Frasnian
153 samples in order to constrain the stratigraphic position of the Kellwasser horizons, particularly the less
154 well defined LKW Level. Finally, in order to better understand the degree of hydrographic connectivity
155 between the Chęciny–Zbrza Basin and the global ocean during the Late Devonian, sedimentary
156 molybdenum and uranium enrichment values were ascertained for a combination of the new samples
157 collected for this study and additional material from a third Kowala sample-set, previously described by
158 Bond *et al.* (2004), which collectively spanned the entire stratigraphic sequence from upper Frasnian to
159 upper Famennian strata.

160

161

162 **2. Methods**

163

164 Preparation of samples for Re–Os analysis was performed in the Laboratory for Source Rock
165 Geochronology and Geochemistry at Durham University (UK), utilising carius-tube digestion with

166 $\text{Cr}^{\text{IV}}\text{O}_3\text{-H}_2\text{SO}_4$, and Os purification using solvent extraction (by chloroform) and microdistillation
167 techniques, following the procedure in Selby and Creaser (2003). Re purification was carried out by
168 anion chromatography following treatment with NaOH and acetone (after Cumming *et al.*, 2013).
169 Isotope compositions and concentrations of Re and Os were determined by isotope dilution and
170 negative thermal ionisation mass spectrometry (N-TIMS) on a ThermoScientific Triton in the Arthur
171 Holmes Laboratory at Durham University. In-house standards were used to monitor analytical
172 reproducibility (see Nowell *et al.*, 2008; and supplementary information in Du Vivier *et al.*, 2014). The
173 $^{187}\text{Os}/^{188}\text{Os}$ and $^{187}\text{Re}/^{185}\text{Re}$ values generated during sample analysis were 0.16077 ± 0.00032 (1 σ) and
174 0.59777 ± 0.00147 (1 σ), respectively, consistent with running averages for the laboratory (see
175 Supplementary Tables).

176
177 All other accompanying geochemical analyses were undertaken at the University of Lausanne
178 (Switzerland). Total organic carbon (TOC) analyses were performed on bulk rock samples using a Rock
179 Eval 6 (see Behar *et al.*, 2001). New $\delta^{13}\text{C}$ data were generated as described in Fantasia *et al.* (2018a).
180 Carbonate $\delta^{13}\text{C}$ ($\delta^{13}\text{C}_{\text{carb}}$) compositions were ascertained using a Thermo Fisher Scientific Gas Bench II
181 connected to a Delta Plus XL isotope ratio mass spectrometer, following reaction of precisely weighed
182 aliquots of powdered samples with anhydrous phosphoric acid at 70 °C. Bulk organic-matter $\delta^{13}\text{C}$
183 ($\delta^{13}\text{C}_{\text{org}}$) compositions were determined on aliquots of samples that had been decarbonated using 10%
184 HCl and subsequently rinsed multiple times with deionized water and milli-Q purified water to restore a
185 neutral pH and dried at 40 °C, using flash combustion on a Carlo Erba 1108 elemental analyser
186 connected to a Thermo Fisher Scientific Delta V isotope ratio mass spectrometer. Analytical uncertainty
187 was ± 0.06 ‰ (1 σ) for $\delta^{13}\text{C}_{\text{carb}}$, as determined by repeated measurements of a Carrara marble internal
188 standard (7 per 45 unknown samples), and ± 0.15 ‰ (1 σ) for $\delta^{13}\text{C}_{\text{org}}$, based on analyses of internal
189 laboratory and international standards.

190
191 Aluminium abundances were established via X-ray fluorescence (XRF) of fused lithium
192 tetraborate glass discs, using a PANalytical PW2400 spectrometer. To create the glass discs, 2.5–3 g
193 (depending on the carbonate content) of powdered bulk sample was measured and its precise mass

194 determined. The weighed samples were baked at 1050 °C for 3 hours, weighed again to ascertain the
195 mass lost during calcination, and re-powdered. Exactly 1.2 g of the new powder was mixed with
196 precisely 6 g of Li₂B₄O₇ material, and the resultant mixture heated in a platinum crucible at 550 °C for
197 10 minutes to form a fused lithium tetraborate glass disc. The glass was left to cool for at least 5
198 minutes before being labelled for identification during analysis. The analytical uncertainty of this
199 technique has been shown previously to be lower than ±5% (Fantasia *et al.*, 2018b).

200
201 Molybdenum (⁹⁵Mo) and uranium (²³⁸U) contents were determined by laser-ablation inductively
202 coupled plasma-mass spectrometry (LA-ICP-MS) on fragments of the glass discs used for XRF analysis
203 (see above). Analysis was conducted using an Element XR sector-field ICP-mass spectrometer
204 interfaced to a NewWave UP-193 ArF excimer ablation system, which fired a 150 µm diameter laser
205 beam with 5 J/cm² on-sample energy density at a repetition rate of 10 Hz. A 90 second background was
206 taken before three separate firings of the laser (of 50 seconds duration, with 15–20 seconds between
207 each firing). CaO wt% obtained by XRF analysis (see above) was used as an internal standard, with a
208 sample of NIST-SRM612 glass employed as an external standard. Data reduction was carried out using
209 LAMTRACE software (Longerich *et al.*, 1996), with reproducibility generally within ±5% for Mo and
210 ±1% for U (1 σ). Full geochemical data are presented in the Supplementary Tables.

211

212

213 **3. Results**

214

215 A clear increase in TOC content, correlative with positive excursions in δ¹³C values of both
216 carbonates and bulk organic-matter, is recorded 2 m below the F–F boundary (Figure 3). These trends
217 are consistent with previous findings (Joachimski *et al.*, 2001), and, when combined with
218 biostratigraphic information (Racki *et al.*, 2002), are likewise interpreted as indicating the position of
219 the UKW Horizon in the absence of the bituminous shales that typically define the Kellwasser levels in
220 western Europe. An additional set of organic-rich shale layers is also observed 11–12 m below the F–F
221 boundary (~10 m below the base of the UKW Horizon), which is marked by elevated TOC contents and

222 an enrichment in both uranium and molybdenum concentrations (Figure 3). These results indicate that a
223 brief period of marine anoxia occurred in this area prior to, and distinct from, the UKW Event. This
224 level is tentatively interpreted as marking the LKW Horizon. Whilst the absence of biostratigraphic
225 information in the new sample set means that it cannot be verified that this shale layer assumed to be
226 the LKW Horizon occurs within the *Late rhenana* Zone, the position of the level 11–12 m below the
227 base of the F–F boundary matches the biostratigraphic and chemostratigraphic positioning of the LKW
228 at Kowala by Joachimski *et al.* (2001). No positive excursion in either $\delta^{13}\text{C}_{\text{carb}}$ or $\delta^{13}\text{C}_{\text{org}}$ is documented
229 at this stratigraphic level, similarly to Joachimski *et al.* (2001) who found only a very minor increase in
230 $\delta^{13}\text{C}_{\text{carb}}$ values and a single-data-point positive excursion in $\delta^{13}\text{C}_{\text{org}}$ at their inferred LKW Horizon 12 m
231 below the F–F boundary. In the absence of a positive $\delta^{13}\text{C}$ excursion, or detailed conodont
232 biostratigraphy for the new samples, the inferred LKW horizon in this study cannot be stratigraphically
233 correlated with other Late Devonian records, and it cannot be ruled out that this level actually marks a
234 spell of localized anoxia that was unrelated to the LKW Event. Nevertheless, the similarity in
235 geochemical perturbations and stratigraphic position (relative to the F–F boundary) of the layer
236 interpreted as the LKW Horizon here compared to the LKW shale at Kowala established by previous
237 studies (Joachimski *et al.*, 2001; Racki *et al.*, 2002) means that it is not unreasonable to assume that this
238 episode of marine anoxia prior to the UKW Event was indeed the local manifestation of the LKW
239 crisis. This interpretation is followed hereafter in the results and discussion.

240
241 Variations in the enrichment trends of Mo and U throughout upper Frasnian to upper
242 Famennian strata match the patterns expected in a marine basin where the drawdown of molybdenum is
243 dominated by particulate shuttling (Figure 4). This system of molybdenum scavenging relies on a
244 reducing water column. Consequently, it is most prevalent today in marine basins that are at least semi-
245 restricted hydrographically with respect to the global ocean (Algeo and Tribovillard, 2009; see also
246 Algeo and Howe, 2012, and references therein), which has also been proposed for various marine
247 basins from other times in Earth's history (Tribovillard *et al.*, 2012), although reducing settings
248 dominated by upwelling have also been shown to feature particulate-shuttle drawdown of molybdenum
249 (Zheng *et al.*, 2000).

250
251 Stratigraphic trends in $Os_{(i)}$ from Kowala are shown in Figure 2A, where the succession has
252 been split into six divisions (A–F) to aid interpretation. Background $Os_{(i)}$ values of the two lowest
253 Frasnian samples from below the inferred LKW Horizon (division A) and Famennian samples between
254 the UKW and Annulata horizons (division E) are relatively consistent: typically between 0.4–0.5 (mean
255 ~ 0.52). Contrastingly, there are significant deviations from this background in $Os_{(i)}$ values across the
256 two Kellwasser horizons and the Annulata shales. The base of the LKW Horizon records a very
257 radiogenic $Os_{(i)}$ value of ~ 0.93 , and another peak at ~ 0.73 just below that level, separated by a return to
258 near background values (division B). The upper part of the LKW Horizon documents a much more
259 unradiogenic $Os_{(i)}$ composition of ~ 0.21 , and a very high content of common osmium (represented as
260 ^{192}Os), albeit based on analysis of just one sample. $Os_{(i)}$ compositions between the two Kellwasser
261 horizons also fluctuate, but to a lesser extent (division C), with both somewhat unradiogenic and a
262 slightly radiogenic value documented, relative to the Late Devonian background. Just below the UKW
263 horizon there is a second increase in $Os_{(i)}$ values from ~ 0.31 to a peak of ~ 0.81 (division D). The
264 remainder of samples from the UKW Horizon have a relatively consistent $Os_{(i)}$ composition of ~ 0.40 ,
265 comparable to the Late Devonian background (division D), except for the sample closest to the F–F
266 boundary itself, which has an anomalous $Os_{(i)}$ value of -0.25 . Above the UKW Horizon, Famennian
267 samples also show relatively consistent $Os_{(i)}$ values of 0.45 – 0.5 (division E), with only one sample
268 deposited in the *marginifera* Zone recording a more radiogenic $Os_{(i)}$ composition of 0.73 . Just below
269 and above the Annulata shales rather unradiogenic $Os_{(i)}$ values of ~ 0.2 and ~ 0.35 are documented,
270 respectively, but there is a more radiogenic composition of ~ 0.53 in the main body of the Annulata
271 shales (division F). A large variability in $Os_{(i)}$ values was also documented in the four samples from the
272 Hangenberg Level, but no clear trend is shown, and two of the four samples recorded compositions well
273 outside the expected range of 0.13 to 1.4 for an open-marine setting (0.06 and -0.91 ; Supplementary
274 Figure 1).
275
276

277 4. Discussion

278

279 4.1. Comparison of Kowala Os-isotope values with North American records

280

281 Only one sedimentary horizon from significantly below the Kellwasser horizons at Kowala was
282 investigated for this study, with an $Os_{(i)}$ ratio of 0.61 in the mid Frasnian *punctata* conodont Zone
283 (Figure 2). In contrast, Re–Os isochron data from the only previously studied sedimentary layer that
284 was deposited prior to the LKW Event (from Pecos County Well of the Permian Basin in Texas, USA)
285 recorded a value of 0.29 (Harris *et al.*, 2013). However, this discrepancy in pre-LKW $Os_{(i)}$ values
286 between Kowala and Texas might be because the studied sediments are not time equivalent, as the
287 limited biostratigraphic constraints on the Pecos County Well hinders stratigraphic correlation of that
288 record with those from elsewhere. Therefore, it is currently difficult to constrain a true global-ocean Os-
289 isotope composition for the Frasnian prior to the Kellwasser crises.

290

291 North American Os-isotope studies of the F–F boundary and sediments just above (uppermost
292 *linguiformis* – *marginifera* Zones), across multiple stratigraphic sequences, indicate a global-ocean Os-
293 isotope composition of 0.4–0.5 at the end of the Frasnian Stage and during the earliest Famennian
294 (Figure 2B; see Turgeon *et al.*, 2007; Gordon *et al.*, 2009; Harris *et al.*, 2013). These values are broadly
295 consistent with the results from within UKW and lowermost Famennian strata at Kowala (Figure 2),
296 suggesting that sediments from both Kowala and the North American records were deposited in marine
297 settings where water masses were well mixed with the global ocean. The Late Devonian $Os_{(i)}$ average
298 from North America (~0.46) is also very similar to the Os-isotope compositions recorded in Frasnian–
299 Famennian boundary and lower–mid Famennian strata at Kowala, supporting this hypothesis. An
300 elevated $Os_{(i)}$ value of 0.59 from an upper Famennian level in the Permian Basin might be equivalent to
301 the shift towards more radiogenic compositions recorded at the top of the *marginifera* Zone at Kowala
302 (Figure 2; Harris *et al.*, 2013), although it cannot be conclusively demonstrated that these stratigraphic
303 levels are the same age due to the lack of biostratigraphy in the Permian Basin record. It should be
304 noted that both here, and in previous studies, Famennian $Os_{(i)}$ information is at low resolution, and more

305 detailed studies of early–mid Famennian shales (as done here for the Kellwasser and Annulata beds) are
306 needed to confirm that the global ocean did indeed experience no short-term changes in its Os-isotope
307 composition over millions of years. Nonetheless, the broad agreement in $Os_{(i)}$ trends across the F–F
308 boundary and lower–mid Famennian strata from Kowala and North America is suggestive that the
309 Chęciny–Zbrza Basin was sufficiently hydrographically well connected to the open ocean with respect
310 to osmium to record the global seawater Os-isotope signature during that time interval, despite
311 indications from the trends in sedimentary Mo and U enrichment factors that water-mass exchange
312 into/out of the basin could have been at least semi-restricted (Figure 4). Apparently semi-restricted
313 basins that record $Os_{(i)}$ trends broadly consistent with changes in the global ocean have been previously
314 reported (e.g., the Toarcian record from the Cleveland Basin, UK; see Cohen *et al.*, 2004; Percival *et*
315 *al.*, 2016; Them *et al.*, 2017); so the possibility of a global ocean $Os_{(i)}$ signature being recorded at
316 Kowala is not inconsistent with the Mo and U evidence of semi-restriction.

317
318 Moreover, both of the Kellwasser crises are thought to have featured significant marine
319 transgressions at their onsets, with a large regression following the UKW crisis (e.g., Johnson *et al.*,
320 1985; Bond and Wignall, 2008). If this was the case, then sea levels should have been higher during the
321 transgressions of the two Kellwasser crises than in Famennian times that followed the post-Kellwasser
322 regression. Higher sea levels should have resulted in an increased hydrographic connectivity between
323 marine-shelf basins and the global ocean. Therefore, given that lower–mid Famennian strata at Kowala
324 appear to record the global-ocean $^{187}Os/^{188}Os$ composition, it would be expected that a similarly open-
325 marine signature should also be documented by sediments deposited during the Kellwasser crises, when
326 sea levels were higher than during the Famennian.

327
328 The results from the Hangenberg shales and Devonian–Carboniferous boundary interval at
329 Kowala (see Supplementary Figure 1) do not agree with a previously published $Os_{(i)}$ value of 0.42 from
330 the D–C boundary in North America (Selby and Creaser, 2005). Of the four stratigraphic layers that
331 were studied from that interval at Kowala, two document $Os_{(i)}$ compositions outside the expected range
332 for the open ocean (0.13–1.4), and none match the North American value of 0.42. However, there is

333 evidence of potential trace-metal content alteration in strata at the top of the Kowala Quarry (where the
334 Hangenberg shales and D–C boundary are recorded; Marynowski *et al.*, 2017) via weathering of those
335 sediments, which could have remobilized the Re and Os in those sediments and caused the anomalous
336 $Os_{(i)}$ values (Peucker-Ehrenbrink and Hanningan, 2000). A similar problem might also be responsible
337 for the single anomalous data point at the F–F boundary, where it has been previously noted that some
338 sediments appear to have been oxidized by groundwater or hydrothermal fluids (see Racki *et al.*, 2002;
339 Bond *et al.*, 2004). However, the sample in question does not appear to show the same discolouration as
340 mentioned in those studies.

341

342

343 4.2. Globally enhanced weathering rates during the Frasnian–Famennian transition

344

345 If the sediments at Kowala are correctly interpreted as recording the $^{187}Os/^{188}Os$ composition of
346 the open ocean, the significant variations observed in $Os_{(i)}$ values from Frasnian–Famennian boundary
347 strata at that location should reflect changes in the inputs of osmium to that inventory. Consequently,
348 whilst $Os_{(i)}$ values from uppermost Frasnian and lower–mid Famennian strata indicate a relatively
349 consistent global-ocean Os-isotope composition, a shift towards more radiogenic signatures just below
350 the UKW Horizon suggests that the marine realm experienced an influx of relatively radiogenic
351 osmium (or a reduction in primitive osmium input) immediately prior to that event. The shifts towards
352 radiogenic $Os_{(i)}$ values in the lower part of and a little below the LKW Horizon may reflect a similar
353 phenomenon taking place before/during the earlier crisis, assuming that the interpreted position of the
354 LKW Horizon is correct. However, because there is also a return to near-background $Os_{(i)}$ within the
355 more radiogenic values below the LKW Horizon, it is not clear whether these data represent two
356 distinct weathering pulses, or a single pulse partially offset by a coeval influx of unradiogenic osmium.
357 However, in either case, the two radiogenic values within/below LKW strata are suggestive of an
358 increased influx of terrigenous material in the lead up to that crisis. It should be noted though that the
359 inferred hypothesis of radiogenic osmium input is based on only two or three data points for both crises,
360 and should be confirmed by additional higher resolution studies, particularly for the LKW Event.

361

362 The most plausible explanation for the increases in global-ocean $\text{Os}_{(i)}$ seawater values at the
363 onsets of the two Kellwasser events is a large influx of radiogenic Os derived from enhanced
364 continental weathering rates at those times. This hypothesis is consistent with elemental ratios such as
365 titanium/aluminium, silicon/aluminium, and zirconium/rubidium from numerous other F–F marine
366 records that indicate an increased detrital influx from the continents (e.g., Pujol *et al.*, 2006; Whalen *et*
367 *al.*, 2015). Alternatively, a shift towards a more radiogenic $^{187}\text{Os}/^{188}\text{Os}$ signature in the global ocean
368 might signify a large decrease in mid-ocean-ridge volcanism, but such a change would be expected to
369 occur over millions of years, and would be very unlikely to result in the abrupt changes in seawater $\text{Os}_{(i)}$
370 recorded at Kowala, leaving weathering as the more likely cause.

371

372 Interestingly, this interpretation suggests that continental weathering rates were extremely
373 elevated just before and during the onsets of the two Kellwasser crises, but then returned to background
374 levels or below throughout the main body of the two events. This finding is in contrast to detrital-influx
375 and strontium-isotope ($^{87}\text{Sr}/^{86}\text{Sr}$) studies from Europe, North America and South China (Chen *et al.*,
376 2005; Pujol *et al.*, 2006; Whalen *et al.*, 2015), which suggest that weathering rates were enhanced
377 throughout the entirety of the two Kellwasser crises. However, strontium is less suitable than osmium
378 for recording the precise timing and/or duration of geologically abrupt changes to the marine inventory
379 due to the very long oceanic residence time of that element (1–4 Myr; Palmer and Edmond, 1989). A
380 prolonged input of terrigenous detrital input to some basins might indeed have occurred, but could have
381 been local to those areas, and not reflective of global-scale changes in continental weathering. An
382 alternative possibility is that enhanced terrestrial runoff did continue throughout the entirety of the
383 Kellwasser crises, but that following the initial pulse of continental weathering, the radiogenic seawater
384 $\text{Os}_{(i)}$ composition was offset by an influx of primitive osmium related to some form of
385 volcanic/hydrothermal activity or basalt-seawater interaction. Thus, the published Sr-isotope and
386 detrital-influx trends are not necessarily inconsistent with the findings of this study. Consequently, on
387 the basis of the results presented here and in previous studies (Chen *et al.*, 2005; Pujol *et al.*, 2006;
388 Whalen *et al.*, 2015), it is concluded that the most significant pulses of global continental weathering

389 during the Frasnian–Famennian transition began just prior to the two Kellwasser crises, although
390 enhanced terrestrial runoff may have continued in some areas throughout the events.

391
392 A significant increase in global-scale continental weathering rates would likely have resulted in
393 a greatly enhanced delivery of nutrients to the marine realm, elevating primary-productivity levels and
394 consequently stimulating widespread marine anoxia and burial of organic carbon (as previously
395 proposed by e.g., Wilder, 1994; Algeo *et al.*, 1995; Algeo and Scheckler, 1998; Averbuch *et al.*, 2005),
396 which may then have been sustained by remobilization of nutrients from aquatic sediments under those
397 low-oxygen conditions (Murphy *et al.*, 2000). Together with this organic-carbon burial, the enhanced
398 silicate weathering could also have resulted in a drawdown of CO₂ and consequential global cooling,
399 which has also been reported for the two Kellwasser crises (e.g., Joachimski and Buggisch, 2002; Balter
400 *et al.*, 2008; Xu *et al.*, 2012; Le Houedec *et al.*, 2013; Huang *et al.*, 2018). Thus, the pattern of
401 enhanced continental weathering rates immediately prior to/during the onsets of the two Kellwasser
402 crises is consistent with evidence of several other environmental perturbations in effect during those
403 times, and follows a relationship between climate change, continental weathering, and/or marine anoxia
404 that is similar to scenarios proposed for a number of other major events throughout the Phanerozoic
405 Aeon (e.g., Kaiser *et al.*, 2006; Bond and Grasby, 2017; Jenkyns, 2018). Importantly, these findings
406 also support previous proposals that this weathering acted as an important trigger for degradation to the
407 global environment during the Kellwasser events (Algeo and Scheckler, 1998; Averbuch *et al.*, 2005).

408

409

410 *4.3. Possible causes of the Frasnian–Famennian weathering pulses*

411

412 What process or processes initially caused the increase in continental weathering rates remains
413 unclear. Mesozoic Oceanic Anoxic Events (OAEs) have been widely linked to large-scale volcanism,
414 with volcanic CO₂ emissions thought to have triggered atmospheric warming and subsequent increased
415 weathering rates (see review by Jenkyns, 2010). Argon–argon (Ar–Ar) dating of Viluy Trap basalts has
416 indicated a major magmatic pulse of late Frasnian age (~374 Ma; Ricci *et al.*, 2013; Polyansky *et al.*,

417 2017), with widespread volcanic activity also taking place on several tectonic rift-systems during the
418 Late Devonian (reviewed in Kravchinski, 2012). A precise coincidence between this volcanism and the
419 Upper Kellwasser Event has been inferred on the basis of mercury enrichments within UKW strata
420 (Racki *et al.*, 2018). The very high Os concentration and low $Os_{(i)}$ value of 0.21 from the inferred LKW
421 Horizon observed in this study (Figure 3) may also indicate a major input of unradiogenic Os from
422 primitive mantle-derived volcanism during the earlier event; a meteorite impact might also cause these
423 changes in Os concentration and isotopic composition, but evidence for such a phenomenon during the
424 LKW Event is lacking (Claeys *et al.*, 1996; Racki, 1999; Percival *et al.*, 2018). However, it should be
425 noted that this pulse in primitive osmium appears above the shift to radiogenic $Os_{(i)}$ values, which
426 would imply that any volcanism during the LKW Event occurred after the weathering pulse. Moreover,
427 there is currently limited evidence that surface warming occurred during the Kellwasser events; rather,
428 those times appear to have been associated with global cooling (e.g., Joachimski and Buggisch, 2002;
429 Balter *et al.*, 2008; Le Houedec *et al.*, 2013; Huang *et al.*, 2018). Possible negative excursions in
430 conodont oxygen-isotope compositions just below the two Kellwasser horizons might indicate brief
431 warming spells at the onsets of the two crises (see Joachimski and Buggisch, 2002), but these trends are
432 far more ambiguous than the pronounced positive shifts interpreted as cooling signals, and could also
433 have resulted from local salinity changes rather than warming. Better evidence of significant global
434 warming is required in order to satisfactorily link the weathering and marine anoxia during the
435 Kellwasser events to volcanism, unless Late Devonian volcanic activity triggered enhanced global
436 weathering via a profoundly different causal mechanism to that proposed for the Mesozoic OAEs.

437
438 Increased weathering rates related to global cooling events have been recorded as having
439 coincided with the expansion of Cenozoic ice sheets during the Eocene–Oligocene transition and Early–
440 Mid Pliocene (e.g., Blum, 1997; Robert and Kennett, 1997; von Blanckenburg and O’Nions, 1999), as
441 well as throughout the formation of alpine-style glaciers in the Alpine–Himalayan belt (Herman *et al.*,
442 2013). Additionally, continental weathering pulses have been associated with the onset and termination
443 of both the Late Ordovician and Fammenian glaciations, which also occurred broadly coevally with the
444 development of widespread marine anoxia/euxinia and major faunal extinctions (e.g., Finlay *et al.*,

445 2010; Kaiser *et al.*, 2016; Lakin *et al.*, 2016). However, whilst it is clearly possible to trigger enhanced
446 continental weathering and/or marine anoxia during times of cooling and glacial expansion,
447 conclusively demonstrating such a model for the Kellwasser events is inhibited by the lack of clarity
448 regarding the precise temporal relationship between the two crises and the onset of global cooling
449 associated with each of them. Different sedimentary records individually suggest that cooling may have
450 begun before, synchronous with, or after the commencement of marine anoxia and associated increase
451 in the deposition of organic matter (e.g., Joachimski and Buggisch, 2002; Balter *et al.*, 2008; Le
452 Houedec *et al.*, 2013; Huang *et al.*, 2018). Higher resolution temperature and weathering proxy data are
453 needed to clarify whether the Kellwasser cooling occurred in response to elevated silicate weathering
454 and organic-carbon burial during the two crises, or could have initiated those environmental
455 perturbations. An additional problem with the hypothesis of glacially-induced-weathering is that
456 although both a southern-hemisphere ice sheet and additional alpine-style glaciers of latest Famennian
457 age are well documented by diamictite deposits in numerous South American sedimentary basins and
458 the North American Appalachian Basin (e.g., Caputo *et al.*, 1985; Brezinski *et al.*, 2008; Isaacson *et al.*,
459 2008; Lakin *et al.*, 2016), similar sediments spanning the Frasnian–Famennian boundary are unknown.
460 A F–F glaciation event has been proposed in order to account for sea-level changes and oxygen-isotope
461 perturbations recorded in uppermost Frasnian to lowermost Famennian sedimentary archives (e.g.,
462 Streel *et al.*, 2000; Joachimski and Buggisch, 2002), but there is currently no direct evidence for the
463 existence of any such ice volumes of that age.

464
465 Other possible triggers for enhanced continental weathering at the onset of each of the
466 Kellwasser crises include marine transgression (e.g., Bond and Wignall, 2008), tectonic uplift
467 associated with the formation of numerous Late Devonian orogenic belts (Averbuch *et al.*, 2005),
468 evolution of vascular-rooted plants (Algeo and Scheckler, 1998), an acceleration of the hydrological
469 cycle by orbital forcing (De Vleeschouwer *et al.*, 2017), and soil erosion related to the extinction of
470 terrestrial plants (Kaiho *et al.*, 2013). However, the severity of land-plant extinctions during the F–F
471 extinction remains poorly constrained (see Racki, 2005; and references therein). Marine transgressions
472 could have caused significant subaerial and/or submarine erosion of the new coastline, and also brought

473 increased moisture into the continental interior, intensifying the hydrological cycle and increasing
474 riverine runoff, although a markedly wetter climate is inconsistent with the widespread evidence for
475 cooling at those times. Finally, whilst processes such as mountain building and the evolution of
476 vascular-root systems likely caused a gradual elevation in continental weathering rates throughout the
477 Late Devonian (a hypothesis consistent with long-term strontium isotope trends: van Geldern *et al.*,
478 2006), it is less clear whether such processes could have occurred rapidly enough to trigger two distinct,
479 abrupt, and short-lived pulses of increased weathering taking place within a million years of each other.
480 However, long-term volcanism, land-plant expansion, orogenic processes, and repeated marine
481 transgressions could plausibly have increased stress in the global climate system throughout Late
482 Devonian times, leaving it increasingly vulnerable to additional environmental perturbations from more
483 rapid triggers such as orbital forcing (see De Vleeschouwer *et al.*, 2017).

484

485

486 *4.4 Volcanically stimulated weathering and anoxia during the Annulata Event*

487

488 As well as appearing across the Kellwasser horizons, significant variations in $Os_{(i)}$ values are
489 also documented in strata spanning the late Famennian Annulata Event at Kowala (Figure 2A). Just
490 below the organic-rich Annulata shales, there is a pronounced shift from Famennian background $Os_{(i)}$
491 values (between 0.4–0.5) towards a very unradiogenic signature, suggesting an influx of primitive
492 osmium to the global ocean. There is currently no evidence for a meteorite impact at that time;
493 however, the date of the Annulata Event matches the Ar–Ar age of the youngest known pulse of Viluy
494 Trap volcanism (363 Ma; Ricci *et al.*, 2013; Polyansky *et al.*, 2017; Percival *et al.*, 2018), based on a
495 cyclostratigraphic timescale anchored to the precise uranium–lead age of the Devonian–Carboniferous
496 boundary (Myrow *et al.*, 2014). A volcanic cause for the shift to primitive $Os_{(i)}$ in strata immediately
497 below the Annulata shales might also be supported by a low $Os_{(i)}$ value in strata just above that unit,
498 which suggests that there may have been a relatively long-lived flux of primitive osmium to the marine
499 realm, a phenomenon more easily explained by prolonged volcanic activity than two distinct inputs of
500 unradiogenic Os from separate, unrecorded, impacts.

501

502 In this context, it is likely that the rise in $Os_{(i)}$ values within the Annulata shales signifies an
503 influx of radiogenic osmium to the ocean during a weathering pulse, superimposed upon a previously
504 very unradiogenic seawater Os-isotope composition, rather than a simple return to background
505 Famennian conditions as might also be inferred from the similarity of $Os_{(i)}$ values between the Annulata
506 shales and lower Famennian strata. Such an increase in continental weathering rates related to volcanic
507 activity would likely have stimulated anoxic conditions following the mechanism outlined above for the
508 Kellwasser crises, and marine anoxia has been documented as having occurred in a number of marine
509 basins during the Annulata Event (e.g., Walliser, 1996; Bond and Zatoń, 2003; Becker *et al.*, 2004;
510 Racka *et al.*, 2010). Establishing palaeotemperature records for the Annulata Event (in particular,
511 whether this late Famennian crisis was associated with climate warming) will be important for further
512 understanding this proposed causal relationship. Regardless of what initiated the enhanced continental
513 weathering during the Annulata Event, its occurrence coincident with widespread marine anoxia
514 highlights the potential similarities between this environmental perturbation and the earlier Kellwasser
515 crises, perhaps supporting previous hypotheses that the Frasnian–Famennian mass extinction may
516 simply have been related to the most severe manifestation of these phenomena (Bond and Grasby,
517 2017).

518

519

520 **5. Conclusions**

521

522 This study has presented the first stratigraphic osmium-isotope ($^{187}Os/^{188}Os$) dataset spanning a
523 long-term record of Frasnian–Famennian times, including the Kellwasser crises and the later Annulata
524 Event. Seawater $^{187}Os/^{188}Os$ values documented in samples from the Frasnian–Famennian boundary and
525 lower–mid Famennian strata at the Kowala Quarry study area are very similar to previously published
526 results from North America, suggesting that the Os-isotope record presented here reflects the global
527 ocean inventory. A number of variations in reconstructed seawater $^{187}Os/^{188}Os$ values are documented,
528 albeit at low resolution. Significantly radiogenic seawater $^{187}Os/^{188}Os$ compositions recorded just

529 below/at the base of both the Lower and Upper Kellwasser horizons indicate that enhanced continental
530 weathering took place immediately prior to and/or during the onset of both of those crises and
531 potentially caused subsequent environmental degradations such as climate cooling and/or widespread
532 marine anoxia, although alternative interpretations regarding the stratigraphic position of the Lower
533 Kellwasser Horizon at Kowala cannot be discounted. An additional, lower-magnitude, shift in
534 $^{187}\text{Os}/^{188}\text{Os}$ towards radiogenic values within the Annulata shales suggests that high weathering rates
535 were also a feature of that later event. These results are consistent with enhanced continental weathering
536 and associated nutrient runoff as a key contributor towards the development of widespread marine
537 anoxia during both the most severe and other, comparatively minor, Late Devonian environmental
538 perturbations, although the ultimate trigger of these different weathering pulses remains unclear.
539 Further work is needed to confirm the record of these weathering pulses at other Late Devonian
540 sedimentary archives, and to determine whether they were initiated by volcanism, glaciation, or some
541 other cause.

542

543

544 **Acknowledgements**

545

546 We thank Thomas Algeo, Sandra Kaiser, and one anonymous reviewer for their constructive feedback
547 which has allowed important improvements to be made to this manuscript. We greatly appreciate the laboratory
548 assistance given by Jean-Claude Lavanchy, Alexey Ulyanov, Geoff Nowell, Chris Ottley, Nicholas Saintilan,
549 Antonia Hofmann, and Zeyang Liu, and also thank Agnieszka Pisarzowska and Ronnie Guthrie for help collecting
550 geological samples in the field. We gratefully acknowledge the TOTAL Endowment Fund and the Dida
551 Scholarship from CUG Wuhan (D.S.), the National Science Centre – Poland (MAESTRO grant
552 2013/08/A/ST10/00717 to G.R., M.R., and L.M.), the Natural Environment Research Council (grant number
553 NE/J01799X/1 to D.P.G.B.), and the University of Lausanne (L.M.E.P.) for funding.

554

555

556 **References**

557

558 Algeo, T.J. and Rowe, H., 2012, Paleooceanographic applications of trace-metal concentration data. *Chemical*
559 *Geology*, 324, p. 6–18, <https://doi.org/10.1016/j.chemgeo.2011.09.002>.
560

561 Algeo, T.J. and Scheckler, S.E., 1998, Terrestrial-marine teleconnections in the Devonian: links between the
562 evolution of land plants, weathering processes, and marine anoxic events. *Philosophical Transactions of*
563 *the Royal Society B: Biological Sciences*, 353, p. 113–130, <https://doi.org/10.1098/rstb.1998.0195>.
564

565 Algeo, T.J. and Tribovillard, N., 2009, Environmental analysis of paleooceanographic systems based on
566 molybdenum–uranium covariation. *Chemical Geology*, 268, p. 211–225,
567 <https://doi.org/10.1016/j.chemgeo.2009.09.001>.
568

569 Algeo, T.J., Berner, R.A., Maynard, J.B. and Scheckler, S.E., 1995, Late Devonian oceanic anoxic events and
570 biotic crises: “rooted” in the evolution of vascular land plants. *GSA today*, 5, p. 45–66.
571

572 Allègre, C.J., Birck, J.L., Capmas, F. and Courtillot, V., 1999, Age of the Deccan traps using 187 Re–187 Os
573 systematics. *Earth and Planetary Science Letters*, 170, p. 197–204, [https://doi.org/10.1016/S0012-](https://doi.org/10.1016/S0012-821X(99)00110-7)
574 [821X\(99\)00110-7](https://doi.org/10.1016/S0012-821X(99)00110-7).
575

576 Averbuch, O., Tribovillard, N., Devleeschouwer, X., Riquier, L., Mistiaen, B. and Vliet-Lanoe, V., 2005,
577 Mountain building-enhanced continental weathering and organic carbon burial as major causes for
578 climatic cooling at the Frasnian–Famennian boundary (c. 376 Ma)? *Terra nova*, 17, p. 25–34,
579 <https://doi.org/10.1111/j.1365-3121.2004.00580.x>.
580

581 Balter, V., Renaud, S., Girard, C. and Joachimski, M.M., 2008, Record of climate-driven morphological changes
582 in 376 Ma Devonian fossils. *Geology*, 36, p. 907–910, <https://doi.org/10.1130/G24989A.1>.
583

584 Becker, R.T., Ashouri, A.R. and Yazdi, M., 2004, The Upper Devonian Annulata Event in the Shotori Range
585 (eastern Iran). *Neues Jahrbuch für Geologie und Paläontologie-Abhandlungen*, p. 119–143.
586

587 Becker, R.T., Kaiser, S.I. and Aretz, M., 2016, Review of chrono-, litho- and biostratigraphy across the global
588 Hangenberg Crisis and Devonian–Carboniferous Boundary. Geological Society, London, Special
589 Publications, 423, p. 355–386, <https://doi.org/10.1144/SP423.10>.
590

591 Behar, F., Beaumont, V. and de B. Penteado, H.L., 2001, Rock-Eval 6 technology: performances and
592 developments. *Oil & Gas Science and Technology*, 56, p. 111–134,
593 <https://doi.org/10.2516/ogst:2001013>.
594

595 Blum, J.D., 1997, The effect of late Cenozoic glaciation and tectonic uplift on silicate weathering rates and the
596 marine $^{87}\text{Sr}/^{86}\text{Sr}$ record. In *Tectonic uplift and climate change* (p. 259–288), Springer, Boston, MA.
597

598 Bond, D.P.G. and Grasby, S.E., 2017, On the causes of mass extinctions. *Palaeogeography, Palaeoclimatology,*
599 *Palaeoecology*, 478, p. 3–29, <https://doi.org/10.1016/j.palaeo.2016.11.005>.
600

601 Bond, D.P.G. and Wignall, P.B., 2008, The role of sea-level change and marine anoxia in the Frasnian–
602 Famennian (Late Devonian) mass extinction. *Palaeogeography, Palaeoclimatology, Palaeoecology*, 263,
603 p. 107–118, <https://doi.org/10.1016/j.palaeo.2008.02.015>.
604

605 Bond, D.P.G. and Zatoń, M., 2003, Gamma-ray spectrometry across the Upper Devonian basin succession at
606 Kowala in the Holy Cross Mountains (Poland). *Acta Geologica Polonica*, 53, p. 93–99.
607

608 Bond, D.P.G., Wignall, P.B. and Racki, G., 2004, Extent and duration of marine anoxia during the Frasnian–
609 Famennian (Late Devonian) mass extinction in Poland, Germany, Austria and France. *Geological*
610 *Magazine*, 141, p. 173–193, <https://doi.org/10.1017/S0016756804008866>.
611

612 Brezinski, D.K., Cecil, C.B., Skema, V.W. and Stamm, R., 2008, Late Devonian glacial deposits from the eastern
613 United States signal an end of the mid-Paleozoic warm period. *Palaeogeography, Palaeoclimatology,*
614 *Palaeoecology*, 268, p. 143–151, <https://doi.org/10.1016/j.palaeo.2008.03.042>.
615

616 Caputo, M.V., 1985, Late Devonian glaciation in South America. *Palaeogeography, Palaeoclimatology,*
617 *Palaeoecology*, 51, p. 291–317, [https://doi.org/10.1016/0031-0182\(85\)90090-2](https://doi.org/10.1016/0031-0182(85)90090-2).
618

619 Chen, D., Qing, H. and Li, R., 2005, The Late Devonian Frasnian–Famennian (F/F) biotic crisis: insights from
620 $\delta^{13}\text{C}_{\text{carb}}$, $\delta^{13}\text{C}_{\text{org}}$ and $^{87}\text{Sr}/^{86}\text{Sr}$ isotopic systematics. *Earth and Planetary Science Letters*, 235, p.
621 151–166, <https://doi.org/10.1016/j.epsl.2005.03.018>.
622

623 Claeys, P., Kyte, F.T., Herbosch, A. and Casier, J.G., 1996, Geochemistry of the Frasnian-Famennian boundary in
624 Belgium: Mass extinction, anoxic oceans and microtektite layer, but not much iridium? *Geological*
625 *Society of America Special Papers*, 307, p. 491–504.
626

627 Cohen, A.S., Coe, A.L., Harding, S.M. and Schwark, L., 2004, Osmium isotope evidence for the regulation of
628 atmospheric CO_2 by continental weathering. *Geology*, 32, p. 157–160, <https://doi.org/10.1130/G20158.1>.
629

630 Cohen, A.S., Coe, A.L., Bartlett, J.M. and Hawkesworth, C.J., 1999, Precise Re-Os ages of organic-rich mudrocks
631 and the Os isotope composition of Jurassic seawater. *Earth and Planetary Science Letters*, 167, p. 159–
632 173, [https://doi.org/10.1016/S0012-821\(99\)00026-6](https://doi.org/10.1016/S0012-821(99)00026-6).
633

634 Courtillot, V., Kravchinsky, V.A., Quidelleur, X., Renne, P.R. and Gladkochub, D.P., 2010, Preliminary dating of
635 the Viluy traps (Eastern Siberia): Eruption at the time of Late Devonian extinction events? *Earth and*
636 *Planetary Science Letters*, 300, p. 239–245, <https://doi.org/10.1016/j.epsl.2010.09.045>.
637

638 Cumming, V.M., Poulton, S.W., Rooney, A.D. and Selby, D., 2013, Anoxia in the terrestrial environment during
639 the late Mesoproterozoic. *Geology*, 41, p. 583–586, <https://doi.org/10.1130/G34299.1>.
640

641 De Vleeschouwer, D., Rakociński, M., Racki, G., Bond, D.P.G., Sobień, K. and Claeys, P., 2013, The
642 astronomical rhythm of Late-Devonian climate change (Kowala section, Holy Cross Mountains,
643 Poland). *Earth and Planetary Science Letters*, 365, p. 25–37, <https://doi.org/10.1016/j.epsl.2013.01.016>.
644

645 De Vleeschouwer, D., Da Silva, A.C., Sinnesael, M., Chen, D., Day, J.E., Whalen, M.T., Guo, Z. and Claeys, P.,
646 2017, Timing and pacing of the Late Devonian mass extinction event regulated by eccentricity and
647 obliquity. *Nature communications*, 8, <https://doi.org/10.1038/s41467-017-02407-1>.
648

649 Dickson, A.J., Cohen, A.S., Coe, A.L., Davies, M., Shcherbinina, E.A. and Gavrillov, Y.O., 2015, Evidence for
650 weathering and volcanism during the PETM from Arctic and Peri-Tethys osmium isotope records.
651 *Palaeogeography, Palaeoclimatology, Palaeoecology*, 438, p. 300–307,
652 [doi:10.1016/j.palaeo.2015.08.019](https://doi.org/10.1016/j.palaeo.2015.08.019).
653

654 Du, Y., Gong, Y., Zeng, X., Huang, H., Yang, J., Zhang, Z. and Huang, Z., 2008, Devonian Frasnian-Famennian
655 transitional event deposits of Guangxi, South China and their possible tsunami origin. *Science in China*
656 *Series D: Earth Sciences*, 51, p. 1570–1580, <https://doi.org/10.1007/s11430-008-0117-1>.
657

658 Du Vivier, A.D., Selby, D., Sageman, B.B., Jarvis, I., Gröcke, D.R. and Voigt, S., 2014, Marine 187Os/188Os
659 isotope stratigraphy reveals the interaction of volcanism and ocean circulation during Oceanic Anoxic
660 Event 2. *Earth and Planetary Science Letters*, 389, p. 23–33, <https://doi.org/10.1016/j.epsl.2013.12.024>.
661

662 Fantasia, A., Föllmi, K.B., Adatte, T., Spangenberg, J.E. and Mattioli, E., 2018a, Expression of the Toarcian
663 Oceanic Anoxic Event: New insights from a Swiss transect. *Sedimentology*,
664 <https://doi.org/10.1111/sed.12527>.
665

666 Fantasia, A., Föllmi, K.B., Adatte, T., Spangenberg, J.E. and Montero-Serrano, J.C., 2018b, The Early Toarcian
667 oceanic anoxic event: Paleoenvironmental and paleoclimatic change across the Alpine Tethys
668 (Switzerland). *Global and Planetary Change*, 162, p. 53–68,
669 <https://doi.org/10.1016/j.gloplacha.2018.01.008>.
670

671 Finlay, A.J., Selby, D. and Gröcke, D.R., 2010, Tracking the Hirnantian glaciation using Os isotopes. *Earth and*
672 *Planetary Science Letters*, 293, p. 339–348, <https://doi.org/10.1016/j.epsl.2010.02.049>.
673

674 Gordon, G.W., Rockman, M., Turekian, K.K. and Over, J., 2009, Osmium isotopic evidence against an impact at
675 the Frasnian-Famennian boundary. *American Journal of Science*, 309, p. 420–430,
676 <https://doi.org/10.2475/05.2009.03>.
677

678 Harris, N.B., Mnich, C.A., Selby, D. and Korn, D., 2013, Minor and trace element and Re–Os chemistry of the
679 Upper Devonian Woodford Shale, Permian Basin, west Texas: insights into metal abundance and basin
680 processes. *Chemical Geology*, 356, p. 76–93, <https://doi.org/10.1016/j.chemgeo.2013.07.018>.
681

682 Herman, F., Seward, D., Valla, P.G., Carter, A., Kohn, B., Willett, S.D. and Ehlers, T.A., 2013, Worldwide
683 acceleration of mountain erosion under a cooling climate. *Nature*, 504, p. 423–426,
684 <https://doi.org/10.1038/nature12877>.
685

686 Huang, C., Joachimski, M.M. and Gong, Y., 2018, Did climate changes trigger the Late Devonian Kellwasser
687 Crisis? Evidence from a high-resolution conodont $\delta^{18}\text{OPO}_4$ record from South China. *Earth and*
688 *Planetary Science Letters*, 495, p. 174–184, <https://doi.org/10.1016/j.epsl.2018.05.016>.
689

690 Isaacson, P.E., Diaz-Martinez, E., Grader, G.W., Kalvoda, J., Babek, O. and Devuyt, F.X., 2008, Late Devonian–
691 earliest Mississippian glaciation in Gondwanaland and its biogeographic
692 consequences. *Palaeogeography, Palaeoclimatology, Palaeoecology*, 268, p. 126–142,
693 <https://doi.org/10.1016/j.palaeo.2008.03.047>.
694

695 Jenkyns, H.C., 2010, Geochemistry of Oceanic Anoxic Events. *Geochemistry Geophysics Geosystems*, 11,
696 Q03004, <https://doi.org/10.1029/2009GC002788>.
697

698 Jenkyns, H.C., 2018, Transient cooling episodes during Cretaceous Oceanic Anoxic Events with special reference
699 to OAE 1a (Early Aptian). *Philosophical Transactions of the Royal Society A: Mathematical, Physical*
700 *and Engineering Sciences*, 376, <https://doi.org/10.1098/rsta.2017.0073>.
701

702 Joachimski, M.M. and Buggisch, W., 1993, Anoxic events in the late Frasnian—Causes of the Frasnian-
703 Famennian faunal crisis? *Geology*, 21, p. 675–678, [https://doi.org/10.1130/0091-](https://doi.org/10.1130/0091-7613(1993)021<0675:AEITLF>2.3.CO;2)
704 [7613\(1993\)021<0675:AEITLF>2.3.CO;2](https://doi.org/10.1130/0091-7613(1993)021<0675:AEITLF>2.3.CO;2).

705
706 Joachimski, M.M. and Buggisch, W., 2002, Conodont apatite $\delta^{18}\text{O}$ signatures indicate climatic cooling as a
707 trigger of the Late Devonian mass extinction. *Geology*, 30, p. 711–714, [https://doi.org/10.1130/0091-](https://doi.org/10.1130/0091-7613(2002)030<0711:CAOSIC>2.0.CO;2)
708 [7613\(2002\)030<0711:CAOSIC>2.0.CO;2](https://doi.org/10.1130/0091-7613(2002)030<0711:CAOSIC>2.0.CO;2).
709
710 Joachimski, M.M., Ostertag-Henning, C., Pancost, R.D., Strauss, H., Freeman, K.H., Littke, R., Damsté, J.S.S.
711 and Racki, G., 2001, Water column anoxia, enhanced productivity and concomitant changes in $\delta^{13}\text{C}$ and
712 $\delta^{34}\text{S}$ across the Frasnian–Famennian boundary (Kowala—Holy Cross Mountains/Poland). *Chemical*
713 *Geology*, 175, p. 109–131, [https://doi.org/10.1016/S0009-2541\(00\)00365-X](https://doi.org/10.1016/S0009-2541(00)00365-X).
714
715 Johnson, J.G., Klapper, G. and Sandberg, C.A., 1985, Devonian eustatic fluctuations in Euramerica. *Geological*
716 *Society of America Bulletin*, 96, p. 567–587, [https://doi.org/10.1130/0016-](https://doi.org/10.1130/0016-7606(1985)96<567:DEFIE>2.0.CO;2)
717 [7606\(1985\)96<567:DEFIE>2.0.CO;2](https://doi.org/10.1130/0016-7606(1985)96<567:DEFIE>2.0.CO;2).
718
719 Kaiho, K., Yatsu, S., Oba, M., Gorjan, P., Casier, J.G. and Ikeda, M., 2013, A forest fire and soil erosion event
720 during the Late Devonian mass extinction. *Palaeogeography, Palaeoclimatology, Palaeoecology*, 392, p.
721 272–280, <https://doi.org/10.1016/j.palaeo.2013.09.008>.
722
723 Kaiser, S.I., Steuber, T., Becker, R.T. and Joachimski, M.M., 2006, Geochemical evidence for major
724 environmental change at the Devonian–Carboniferous boundary in the Carnic Alps and the Rhenish
725 Massif. *Palaeogeography, Palaeoclimatology, Palaeoecology*, 240, p. 146–160,
726 <https://doi.org/10.1016/j.palaeo.2006.03.048>.
727
728 Kaiser, S.I., Aretz, M. and Becker, R.T., 2016, The global Hangenberg Crisis (Devonian–Carboniferous
729 transition): review of a first-order mass extinction. *Geological Society, London, Special*
730 *Publications*, 423, p. 387–437, <https://doi.org/10.1144/SP423.9>.
731
732 Kravchinsky, V.A., 2012, Paleozoic large igneous provinces of Northern Eurasia: correlation with mass extinction
733 events. *Global and Planetary Change*, 86, p. 31–36, <https://doi.org/10.1016/j.gloplacha.2012.01.007>.
734

735 Lakin, J.A., Marshall, J.E.A., Troth, I. and Harding, I.C., 2016, Greenhouse to icehouse: a biostratigraphic review
736 of latest Devonian–Mississippian glaciations and their global effects. Geological Society, London,
737 Special Publications, 423, p. 439-464, <https://doi.org/10.1144/SP423.12>.
738

739 Le Houedec, S., Girard, C. and Balter, V., 2013, Conodont Sr/Ca and $\delta^{18}\text{O}$ record seawater changes at the
740 Frasnian–Famennian boundary. *Palaeogeography, Palaeoclimatology, Palaeoecology*, 376, p. 114–121,
741 <https://doi.org/10.1016/j.palaeo.2013.02.025>.
742

743 Longerich, H.P., Jackson, S.E. and Günther, D., 1996, Inter-laboratory note. Laser ablation inductively coupled
744 plasma mass spectrometric transient signal data acquisition and analyte concentration calculation. *Journal*
745 *of Analytical Atomic Spectrometry*, 11, p. 899–904, <http://doi.org/10.1039/JA9961100899>.
746

747 Marynowski, L., Zatoń, M., Rakociński, M., Filipiak, P., Kurkiewicz, S. and Pearce, T.J., 2012, Deciphering the
748 upper Famennian Hangenberg Black Shale depositional environments based on multi-proxy
749 record. *Palaeogeography, Palaeoclimatology, Palaeoecology*, 346, p. 66–86,
750 <https://doi.org/10.1016/j.palaeo.2012.05.020>.
751

752 Marynowski, L., Piszczowska, A., Derkowski, A., Rakociński, M., Szaniawski, R., Środoń, J. and Cohen, A.S.,
753 2017, Influence of palaeoweathering on trace metal concentrations and environmental proxies in black
754 shales. *Palaeogeography, palaeoclimatology, palaeoecology*, 472, p. 177–191,
755 <https://doi.org/10.1016/j.palaeo.2017.02.023>.
756

757 Murphy, A.E., Sageman, B.B. and Hollander, D.J., 2000, Eutrophication by decoupling of the marine
758 biogeochemical cycles of C, N, and P: A mechanism for the Late Devonian mass
759 extinction. *Geology*, 28, p. 427–430, [https://doi.org/10.1130/0091-](https://doi.org/10.1130/0091-7613(2000)28<427:EBDOTM>2.0.CO;2)
760 [7613\(2000\)28<427:EBDOTM>2.0.CO;2](https://doi.org/10.1130/0091-7613(2000)28<427:EBDOTM>2.0.CO;2).
761

762 Myrow, P.M., Ramezani, J., Hanson, A.E., Bowring, S.A., Racki, G. and Rakociński, M., 2014, High-precision
763 U–Pb age and duration of the latest Devonian (Famennian) Hangenberg event, and its implications. *Terra*
764 *Nova*, 26, p. 222–229, <https://doi.org/10.1111/ter.12090>.
765

766 Nowell, G.M., Luguet, A., Pearson, D.G. and Horstwood, M.S.A., 2008, Precise and accurate 186Os/188Os and
767 187Os/188Os measurements by multi-collector plasma ionisation mass spectrometry (MC-ICP-MS) part
768 I: Solution analyses. *Chemical Geology*, 248, p. 363–393,
769 <https://doi.org/10.1016/j.chemgeo.2007.10.020>.
770

771 Paquay, F.S. and Ravizza, G., 2012, Heterogeneous seawater ¹⁸⁷Os/¹⁸⁸Os during the late Pleistocene
772 glaciations. *Earth and Planetary Science Letters*, 349, p. 126-138,
773 <https://doi.org/10.1016/j.epsl.2012.06.051>.
774

775 Palmer, M.R., Edmond, J.M., 1989, The strontium isotope budget of the modern ocean. *Earth and Planetary*
776 *Science Letters* 92, 11–26, [https://doi.org/10.1016/0012-821X\(89\)90017-4](https://doi.org/10.1016/0012-821X(89)90017-4).
777

778 Percival, L.M.E., Cohen, A.S., Davies, M.K., Dickson, A.J., Hesselbo, S.P., Jenkyns, H.C., Leng, M.J., Mather,
779 T.A., Storm, M.S. and Xu, W., 2016, Osmium isotope evidence for two pulses of increased continental
780 weathering linked to Early Jurassic volcanism and climate change. *Geology*, 44, p. 759–762,
781 <https://doi.org/10.1130/G37997.1>.
782

783 Percival, L.M.E., Davies, J.H.F.L., Schaltegger, U., De Vleeschouwer, D., Da Silva, A.-C. and Föllmi, K.B.,
784 2018, Precisely dating the Frasnian–Famennian boundary: implications for the cause of the Late
785 Devonian mass extinction. *Scientific Reports*, 8, <https://doi.org/10.1038/s41598-018-27847-7>.
786

787 Peucker-Ehrenbrink, B. and Hannigan, R.E., 2000, Effects of black shale weathering on the mobility of rhenium
788 and platinum group elements. *Geology*, 28, p. 475–478, [https://doi.org/10.1130/0091-](https://doi.org/10.1130/0091-7613(2000)28<475:EOBSWO>2.0.CO;2)
789 [7613\(2000\)28<475:EOBSWO>2.0.CO;2](https://doi.org/10.1130/0091-7613(2000)28<475:EOBSWO>2.0.CO;2).
790

791 Peucker-Ehrenbrink, B. and Jahn, B.M., 2001, Rhenium-osmium isotope systematics and platinum group element
792 concentrations: Loess and the upper continental crust. *Geochemistry, Geophysics, Geosystems*, 2,
793 <https://doi.org/10.1029/2001GC000172>.
794

795 Peucker-Ehrenbrink, B. and Ravizza, G., 2000, The marine osmium isotope record. *Terra Nova*, 12, p. 205–219,
796 <https://doi.org/10.1046/j.1365-3121.2000.00295.x>.

797

798 Polyansky, O.P., Prokopiev, A.V., Koroleva, O.V., Tomshin, M.D., Reverdatto, V.V., Selyatitsky, A.Y., Travin,
799 A.V. and Vasiliev, D.A., 2017, Temporal correlation between dyke swarms and crustal extension in the
800 middle Palaeozoic Vilyui rift basin, Siberian platform. *Lithos*, 282, p. 45–64,
801 <https://doi.org/10.1016/j.lithos.2017.02.020>.

802
803 Pujol, F., Berner, Z. and Stüben, D., 2006, Palaeoenvironmental changes at the Frasnian/Famennian boundary in
804 key European sections: Chemostratigraphic constraints. *Palaeogeography, Palaeoclimatology,*
805 *Palaeoecology*, 240, p. 120–145, <https://doi.org/10.1016/j.palaeo.2006.03.055>.

806
807 Racka, M., Marynowski, L., Filipiak, P., Sobstel, M., Piszczowska, A. and Bond, D.P.G., 2010, Anoxic Annulata
808 events in the Late Famennian of the Holy Cross Mountains (Southern Poland): geochemical and
809 palaeontological record. *Palaeogeography, Palaeoclimatology, Palaeoecology*, 297, p. 549–575,
810 <https://doi.org/10.1016/j.palaeo.2010.08.028>.

811
812 Racki, G., 1999, The Frasnian–Famennian biotic crisis: How many (if any) bolide impacts? *Geologische*
813 *Rundschau*, 87, p. 617–632.

814
815 Racki, G., 2005, Toward understanding Late Devonian global events: few answers, many questions.
816 In *Developments in Palaeontology and Stratigraphy*, 20 (p. 5–36) Elsevier.

817
818 Racki, G., Racka, M., Matyja, H. and Devleeschouwer, X., 2002, The Frasnian/Famennian boundary interval in
819 the South Polish–Moravian shelf basins: integrated event-stratigraphical approach. *Palaeogeography,*
820 *Palaeoclimatology, Palaeoecology*, 181, p. 251–297, [https://doi.org/10.1016/S0031-0182\(01\)00481-3](https://doi.org/10.1016/S0031-0182(01)00481-3).

821
822 Racki, G., Rakociński, M., Marynowski, L. and Wignall, P.B., 2018, Mercury enrichments and the Frasnian-
823 Famennian biotic crisis: A volcanic trigger proved? *Geology*, 46, p. 543–546,
824 <https://doi.org/10.1130/G40233.1>.

825

826 Ravizza, G. and Turekian, K.K., 1989, Application of the ^{187}Re - ^{187}Os system to black shale
827 geochronometry. *Geochimica et Cosmochimica Acta*, 53, p. 3257–3262, <https://doi.org/10.1016/0016->
828 [7037\(89\)90105-1](https://doi.org/10.1016/0016-7037(89)90105-1).
829
830 Ricci, J., Quidelleur, X., Pavlov, V., Orlov, S., Shatsillo, A. and Courtillot, V., 2013, New $^{40}\text{Ar}/^{39}\text{Ar}$ and K–Ar
831 ages of the Viluy traps (Eastern Siberia): further evidence for a relationship with the Frasnian–
832 Famennian mass extinction. *Palaeogeography, Palaeoclimatology, Palaeoecology*, 386, p. 531–540,
833 <https://doi.org/10.1016/j.palaeo.2013.06.020>.
834
835 Robert, C. and Kennett, J.P., 1997, Antarctic continental weathering changes during Eocene-Oligocene
836 cryosphere expansion: Clay mineral and oxygen isotope evidence. *Geology*, 25, p. 587–590,
837 [https://doi.org/10.1130/0091-7613\(1997\)025<0587:ACWCDE>2.3.CO;2](https://doi.org/10.1130/0091-7613(1997)025<0587:ACWCDE>2.3.CO;2).
838
839 Rooney, A.D., Selby, D., Lloyd, J.M., Roberts, D.H., Lückge, A., Sageman, B.B. and Prouty, N.G., 2016,
840 Tracking millennial-scale Holocene glacial advance and retreat using osmium isotopes: Insights from the
841 Greenland ice sheet. *Quaternary Science Reviews*, 138, p. 49–61,
842 <https://doi.org/10.1016/j.quascirev.2016.02.021>.
843
844 Rudnick, R.L. and Gao, S., 2003, Composition of the continental crust. In *Treatise on Geochemistry* (p. 1–64),
845 Elsevier, Oxford, U.K., <https://doi.org/10.1016/B0-08-043751-6/03016-4>.
846
847 Selby, D. and Creaser, R.A., 2003, Re–Os geochronology of organic rich sediments: an evaluation of organic
848 matter analysis methods. *Chemical Geology*, 200, p. 225–240, <https://doi.org/10.1016/S0009->
849 [2541\(03\)00199-2](https://doi.org/10.1016/S0009-2541(03)00199-2).
850
851 Selby, D. and Creaser, R.A., 2005, Direct radiometric dating of the Devonian-Mississippian time-scale boundary
852 using the Re–Os black shale geochronometer. *Geology*, 33, p. 545–548,
853 <https://doi.org/10.1130/G21324.1>.
854

855 StreeI, M., Caputo, M.V., Loboziak, S. and Melo, J.H.G., 2000, Late Frasnian–Famennian climates based on
856 palynomorph analyses and the question of the Late Devonian glaciations. *Earth-Science Reviews*, 52, p.
857 121–173, [https://doi.org/10.1016/S0012-8252\(00\)00026-X](https://doi.org/10.1016/S0012-8252(00)00026-X).
858

859 Szulczewski, M., 1971, Upper Devonian conodonts, stratigraphy and faunal development in the Holy Cross
860 Mountains. *Acta Geologica Polonica*, 21, p. 1–129.
861

862 Szulczewski, M., 1996, Devonian succession in the Kowala quarry and railroad cut. In *Sixth European Conodont*
863 *Symposium (ECOS VI), Excursion Guide* (p. 27–30).
864

865 Them, T.R., Gill, B.C., Selby, D., Gröcke, D.R., Friedman, R.M. and Owens, J.D., 2017, Evidence for rapid
866 weathering response to climatic warming during the Toarcian Oceanic Anoxic Event. *Scientific*
867 *reports*, 7, <https://doi.org/10.1038/s41598-017-05307-y>.
868

869 Tribovillard, N., Algeo, T.J., Baudin, F. and Riboulleau, A., 2012, Analysis of marine environmental conditions
870 based on molybdenum–uranium covariation—Applications to Mesozoic paleoceanography. *Chemical*
871 *Geology*, 324, p. 46–58, <https://doi.org/10.1016/j.chemgeo.2011.09.009>.
872

873 Turgeon, S.C., Creaser, R.A. and Algeo, T.J., 2007, Re–Os depositional ages and seawater Os estimates for the
874 Frasnian–Famennian boundary: implications for weathering rates, land plant evolution, and extinction
875 mechanisms. *Earth and Planetary Science Letters*, 261, p. 649–661,
876 <https://doi.org/10.1016/j.epsl.2007.07.031>.
877

878 Van Geldern, R., Joachimski, M.M., Day, J., Jansen, U., Alvarez, F., Yolkin, E.A. and Ma, X.P., 2006, Carbon,
879 oxygen and strontium isotope records of Devonian brachiopod shell calcite. *Palaeogeography,*
880 *Palaeoclimatology, Palaeoecology*, 240, p. 47–67, <https://doi.org/10.1016/j.palaeo.2006.03.045>.
881

882 Von Blanckenburg, F. and O’Nions, R.K., 1999, Response of beryllium and radiogenic isotope ratios in Northern
883 Atlantic Deep Water to the onset of northern hemisphere glaciation. *Earth and Planetary Science*
884 *Letters*, 167, p. 175–182, [https://doi.org/10.1016/S0012-821X\(99\)00028-X](https://doi.org/10.1016/S0012-821X(99)00028-X).
885

- 886 Walliser, O.H., 1996, Global events in the Devonian and Carboniferous. In *Global events and event stratigraphy*
887 *in the Phanerozoic* (p. 225–250), Springer, Berlin, Heidelberg.
- 888
- 889 Wang, K., 1992, Glassy microspherules (microtektites) from an Upper Devonian limestone. *Science*, 256, p.1547–
890 1550, <https://doi.org/10.1126/science.256.5063.1547>.
- 891
- 892 Whalen, M.T., Śliwiński, M.G., Payne, J.H., Day, J.E.J., Chen, D. and Da Silva, A.C., 2015, Chemostratigraphy
893 and magnetic susceptibility of the Late Devonian Frasnian–Famennian transition in western Canada and
894 southern China: implications for carbon and nutrient cycling and mass extinction. *Geological Society*,
895 London, Special Publications, 414, p. 37–72, <https://doi.org/10.1144/SP414.8>.
- 896
- 897 Wilder, H., 1994, Death of Devonian reefs – implications and further investigations. *Courier Forschungsinstitut*
898 *Senckenberg*, 172, p. 241–247.
- 899
- 900 Xu, B., Gu, Z., Wang, C., Hao, Q., Han, J., Liu, Q., Wang, L. and Lu, Y., 2012, Carbon isotopic evidence for the
901 associations of decreasing atmospheric CO₂ level with the Frasnian-Famennian mass extinction. *Journal*
902 *of Geophysical Research: Biogeosciences*, 117, <https://doi.org/10.1029/2011JG001847>.
- 903
- 904 Zheng, Y., Anderson, R.F., van Geen, A. and Kuwabara, J., 2000, Authigenic molybdenum formation in marine
905 sediments: a link to pore water sulfide in the Santa Barbara Basin. *Geochimica et Cosmochimica*
906 *Acta*, 64, p. 4165–4178, [https://doi.org/10.1016/S0016-7037\(00\)00495-6](https://doi.org/10.1016/S0016-7037(00)00495-6).

907

908

909 **Figure Captions**

910

911 **Figure 1:** Palaeogeographic reconstruction of the Late Devonian world. The locations of the Late
912 Frasnian Siljan impact crater (X), and the Frasnian–Famennian Viluy Traps (V) and Kola,
913 Vyatka, and Pripyat–Dniepr–Donets volcanic rift systems (K-V-PDD) are indicated. The
914 palaeogeographic position of the Kowala Quarry, Poland (K) investigated in this study is shown
915 (black circle), along with North American sedimentary records where Re–Os isochrons have

916 been generated previously (black squares): J: Jura Creek (Alberta, Canada; Selby and Creaser,
917 2005); W: West Valley Core (New York, USA; Turgeon *et al.*, 2007); I: Irish Gulf section
918 (New York, USA; Gordon *et al.*, 2009); P: Pecos County Well (Texas, USA; Harris *et al.*,
919 2013). Based on Figure 1 in Percival *et al.* (2018).

920

921 **Figure 2: A:** Stratigraphic trends in $Os_{(i)}$ from the Kowala Quarry record, Kielce, Poland. The
922 stratigraphic positions of the Upper Kellwasser and Annulata levels are shown, along with the
923 inferred Lower Kellwasser Horizon, and the Hangenberg Horizon. Lithological and
924 biostratigraphic information after Szulczewski (1996) and De Vleeschouwer *et al.* (2013). All
925 osmium data are from this study (solid circles). The vertical scale is in metres **B:** Stratigraphic
926 composite of previously published Re–Os isochron data from North American records (open
927 circles). $Os_{(i)}$ data are from Selby and Creaser (2005), Turgeon *et al.* (2007), Gordon *et al.*
928 (2009), and Harris *et al.* (2013). CARB. stands for CARBONIFEROUS. The lowest natural
929 terrestrial value of $^{187}Os/^{188}Os$ (0.13; Allègre *et al.*, 1999) and Late Devonian average seawater
930 $Os_{(i)}$ value (based on North American isochron data) are shown on both figures.

931

932 **Figure 3:** Stratigraphic trends in geochemical data from upper Frasnian sediments at the Kowala
933 Quarry. The interpreted stratigraphic positions of the Lower (LKW) and Upper (UKW)
934 Kellwasser horizons are indicated by the grey bars. Uranium (U) and molybdenum (Mo)
935 enrichment factors (EF) are calculated with respect to Al, relative to average upper continental
936 crust (UCC) abundances as shown by $[(\text{element}/Al)_{\text{sample}}/(\text{element}/Al)_{\text{UCC}}]$, where U/Al_{UCC} and
937 Mo/Al_{UCC} are taken as 0.0000331 and 0.0000135, respectively (Rudnick and Gao, 2003). The
938 lowest natural terrestrial value of $^{187}Os/^{188}Os$ (0.13; Allègre *et al.*, 1999) and Late Devonian
939 average seawater $Os_{(i)}$ value (based on North American isochron data) are plotted alongside the
940 $Os_{(i)}$ data from Kowala. Common ^{192}Os contents are presented as the best representation of Os
941 concentrations in sediments at the time of deposition. The vertical scale is in metres. FM. stands
942 for FAMENNIAN. All data are from this study. Unpublished measurements made in 2011
943 indicate a small enrichment in Mo and U concentrations from samples within the UKW

944 Horizon, but those data were generated via a different methodology to the samples analysed for
945 this study and without accompanying Al contents; therefore, they are not included in this figure
946 (they are presented in Supplementary Figure 2). The enrichment in Mo and U was also
947 observed on UKW Horizon samples from elsewhere in the Kowala Quarry, based on samples
948 from David Bond's 2004 sample-set analysed by LA-ICP-MS for this study (see
949 Supplementary Figure 2), and in previous works (Joachimski *et al.*, 2001; Bond *et al.*, 2004).

950
951 **Figure 4:** Comparison of trends in uranium (U) and molybdenum (Mo) enrichment factors (EF) to
952 determine the palaeoenvironmental setting recorded at the Kowala Quarry, following the model
953 of Algeo and Tribovillard (2009). Mo/U_{SW} indicates the modern-day Mo/U ratio of seawater.
954 Mo_{EF} and U_{EF} data are calculated as for Figure 3. All data are from this study.

Figure 1

Late Devonian (383–359 Ma)

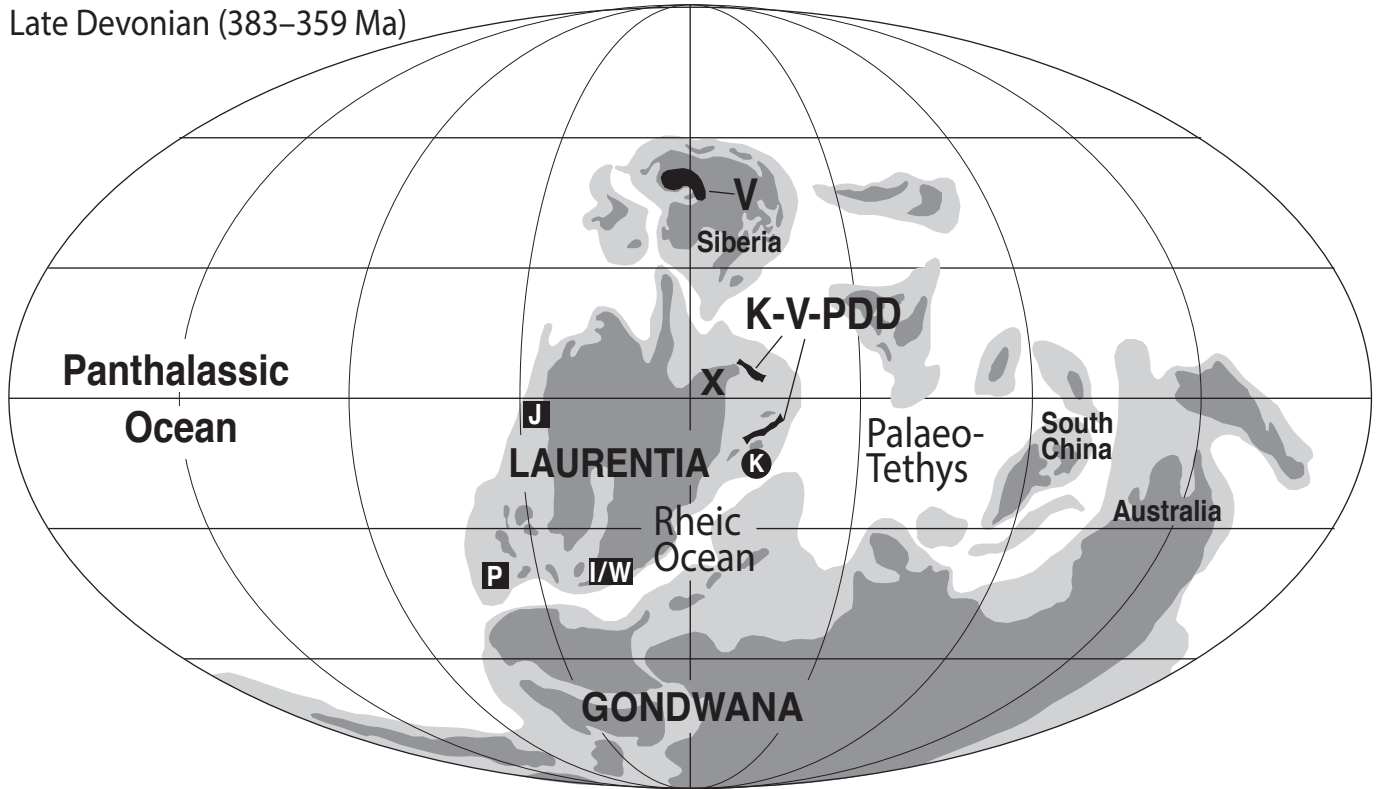
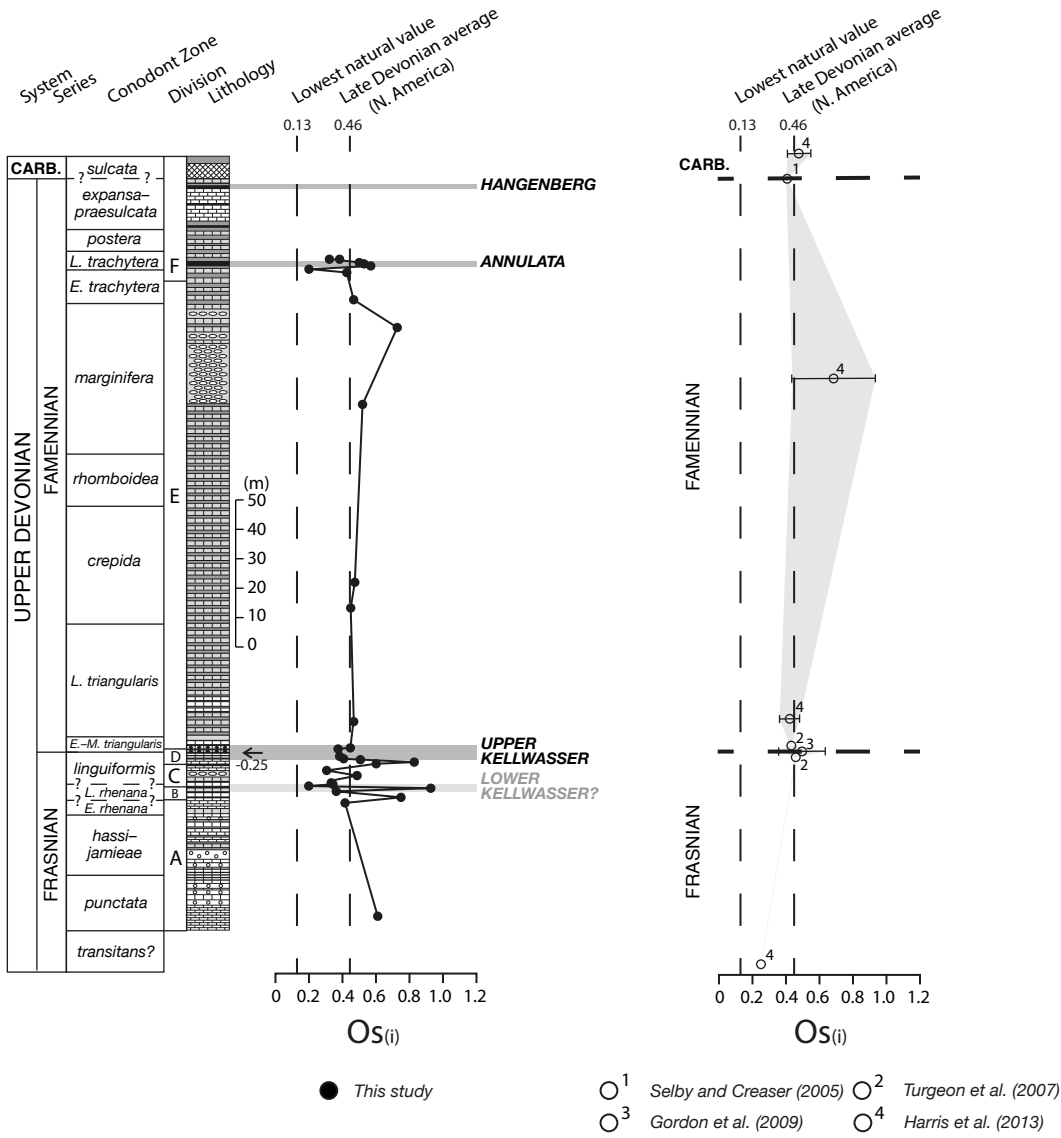


Figure 2

A: Kowala Quarry – this study

B: N. American composite



LITHOLOGY:

- Micritic limestones
- Shales
- Nodular limestones
- Tuffites
- Marls
- Black shales
- Coarse grained limestones
- Cherts

Figure 3

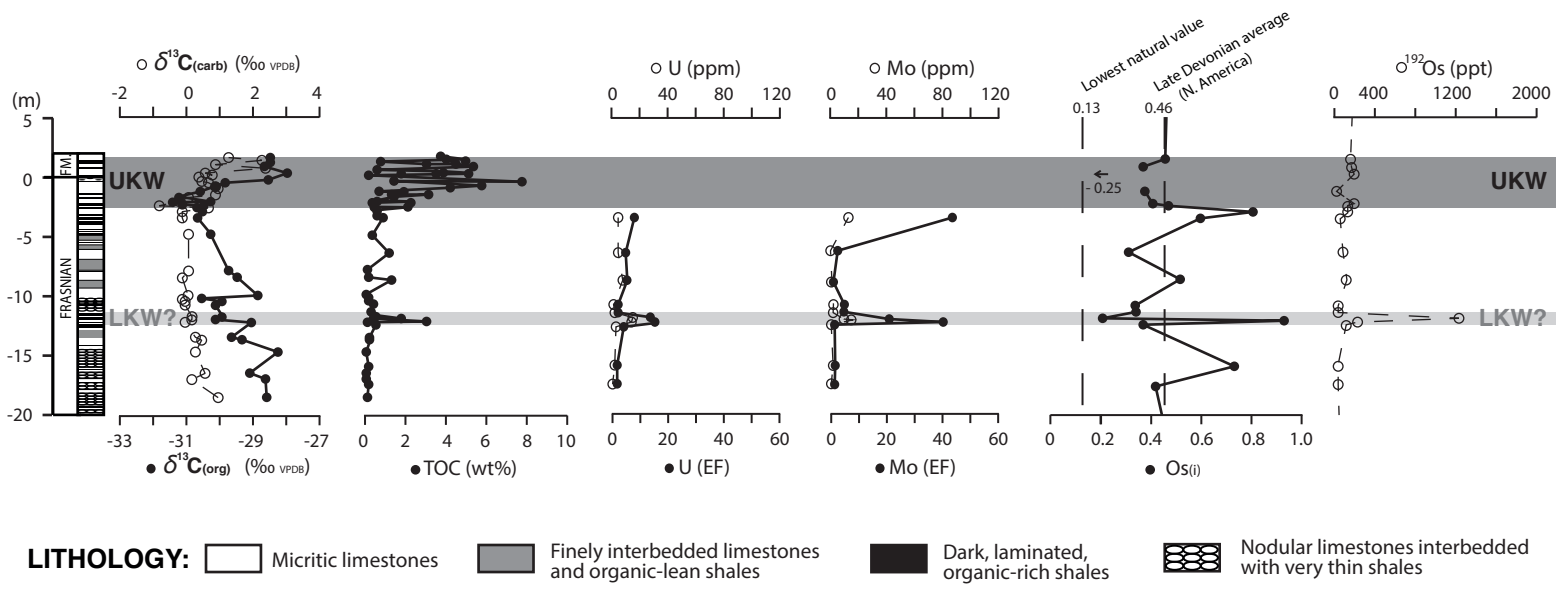
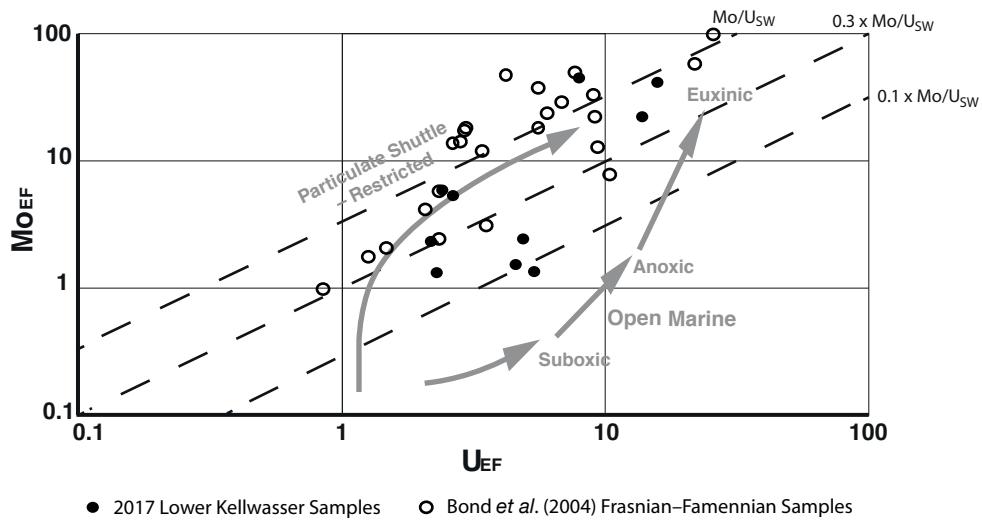
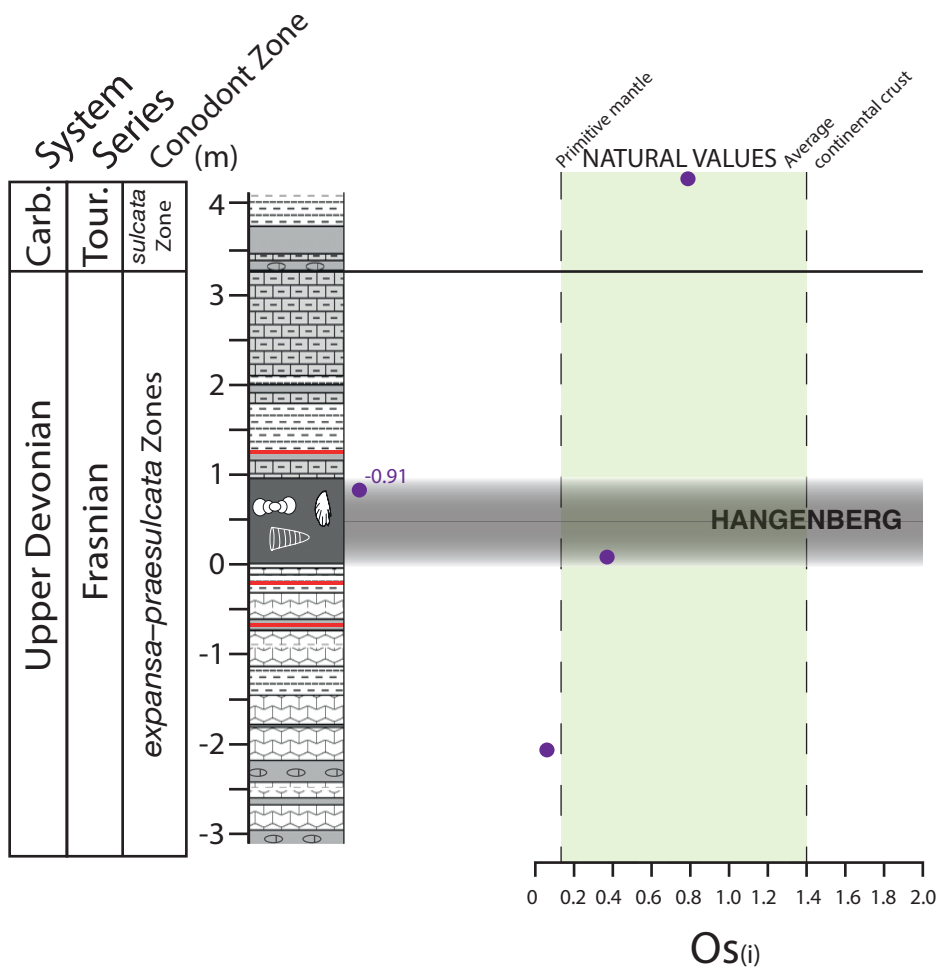


Figure 4



Supplementary Figure 1

HANGENBERG SHALE, KOWALA QUARRY (POLAND) – OSMIUM ISOTOPE RECORD

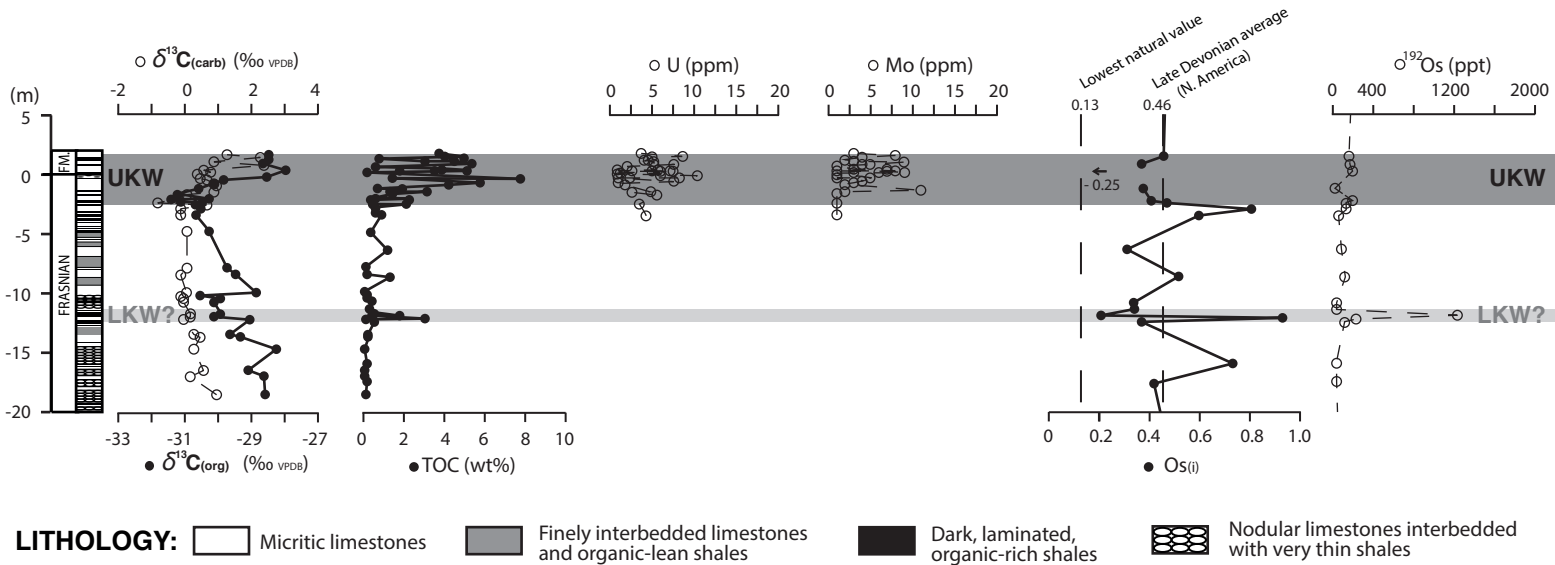


NB. Lithological column and stratigraphic information from Myrow *et al.* (2014). Osmium-isotope data are from this study. Natural range of values of seawater Os(i) features endmembers of 0.13 (primitive mantle volcanics and extra-terrestrial influx; Allégre *et al.*, 1999) and 1.4 (average composition of riverine runoff of upper continental crustal material; Peucker-Ehrenbrink and Jahn, 2001) in the modern, and this range is assumed to have also applied during the Devonian Period.

Supplementary Figure 2

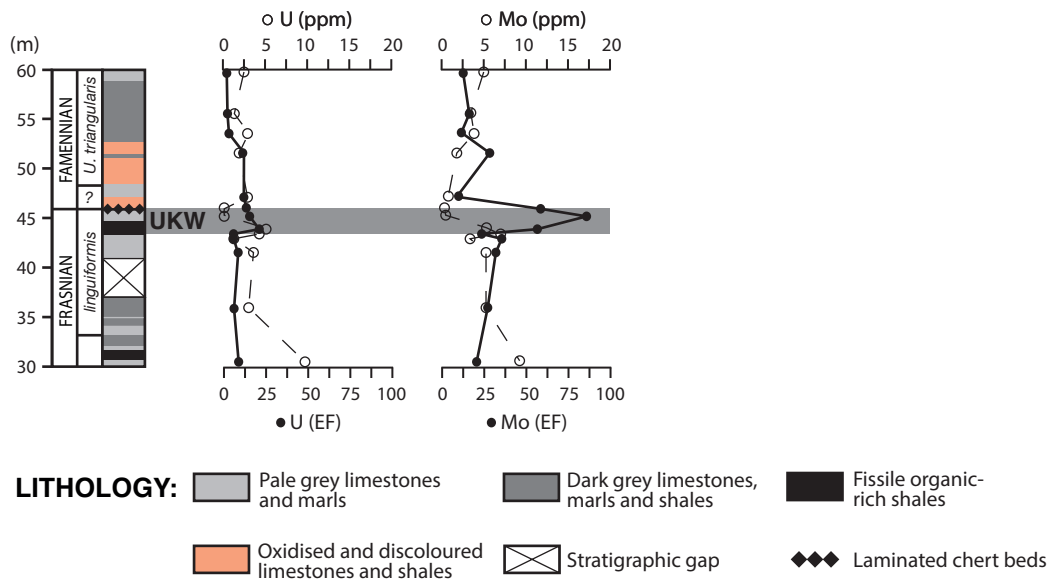
UPPER KELLWASSER HORIZON MOLYBDENUM AND URANIUM RECORDS

University of Sielsia Samples, analysed at Ancaster ACTLabs (Ontario, Canada) in 2011.



Mo and U concentrations were determined by analysis of fused glass discs using a Perkin Elmer Sciex Elemental Analyzer. All other data were generated via the methods described in the main methodology section.

David Bond's 2004 sample set, analysed at the University of Lausanne by LA-ICP-MS (2017).



Samples were collected for Bond et al. (2004). Mo, U, and Al data were generated following the methods outlined in the main methodology section. The samples were taken from a different part of the quarry to the other rocks described in this study, and therefore cannot be easily incorporated on to the same stratigraphic log. Lithological and biostratigraphic information, and the inferred position of the Upper Kellwasser Horizon, are as for Bond et al. (2004).